JACS
JOURNAL OF THE AMERICAN CHEMICAL SOCIETY
Article
pubs.acs.org/JACS

# Identification of an Intermediate Methyl Carrier in the Radical *S*-Adenosylmethionine Methylthiotransferases RimO and MiaB

Bradley J. Landgraf,[†,§] Arthur J. Arcinas,[‡,§] Kyung-Hoon Lee,[†] and Squire J. Booker*[,†,‡]

[†]Department of Chemistry and [‡]Department of Biochemistry and Molecular Biology, The Pennsylvania State University, University Park, Pennsylvania 16802, United States

Supporting Information

**ABSTRACT:** RimO and MiaB are radical *S*-adenosylmethionine (SAM) enzymes that catalyze the attachment of methylthio ($-SCH_3$) groups to macromolecular substrates. RimO attaches a methylthio group at C3 of aspartate 89 of protein S12, a component of the 30*S* subunit of the bacterial ribosome. MiaB attaches a methylthio group at C2 of $N^6$-(isopentenyl)adenosine, found at nucleotide 37 in several prokaryotic tRNAs. These two enzymes are prototypical members of a subclass of radical SAM enzymes called methylthiotransferases (MTTases). It had been assumed that the sequence of steps in MTTase reactions involves initial sulfur insertion into the organic substrate followed by capping of the inserted sulfur atom with a SAM-derived methyl group. In this work, however, we show that both RimO and MiaB from *Thermotoga maritima* catalyze methyl transfer from SAM to an acid/base labile acceptor on the protein in the absence of their respective macromolecular substrates. Consistent with the assignment of the acceptor as an iron−sulfur cluster, denaturation of the SAM-treated protein with acid results in production of methanethiol. When RimO or MiaB is first incubated with SAM in the absence of substrate and reductant and then incubated with excess *S*-adenosyl-L-[*methyl*-$d_3$]methionine in the presence of substrate and reductant, production of the unlabeled product precedes production of the deuterated product, showing that the methylated species is chemically and kinetically competent to be an intermediate.

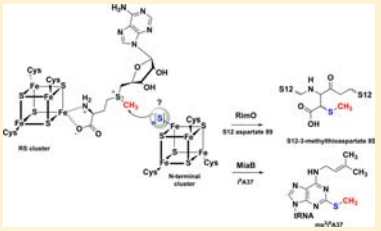

## INTRODUCTION

The radical *S*-adenosylmethionine (SAM)[1] methylthiotransferases (MTTases) catalyze the attachment of methylthio ($-SCH_3$) groups at specific locations on transfer RNAs (tRNAs) or ribosomal proteins, resulting in thioether bonds.[1] Three major classes of MTTases are currently recognized, which are represented by the enzymes MiaB, MtaB, and RimO.[1−3] MiaB catalyzes the final step in the biosynthesis of the hypermodified tRNA nucleoside 2-methylthio-$N^6$-(isopentenyl)adenosine ($ms^2i^6A$), which is the methylthiolation of C2 of $N^6$-(isopentenyl)adenosine ($i^6A$), found at position 37 of certain tRNAs (Scheme 1A), while MtaB catalyzes the methylthiolation of the same carbon center of $N^6$-(threonylcarbamoyl)adenosine ($t^6A$) to afford 2-methylthio-$N^6$-(threonylcarbamoyl)adenosine ($ms^2t^6A$) (Scheme 1B). By contrast, RimO acts on a protein substrate, catalyzing the methylthiolation of the $\beta$-carbon of aspartate 89 [*Escherichia coli* (*Ec*) numbering] of ribosomal protein S12 (Scheme 1C). These proteins, along with biotin synthase (BS) and lipoyl synthase (LS), constitute a special subfamily of radical SAM (RS) enzymes that catalyze sulfur insertion.[1,4−6] All RS enzymes that catalyze sulfur insertion contain two distinct iron−sulfur (Fe/S) clusters: a [4Fe−4S] cluster ligated by cysteines in a $Cx_3Cx_2C$ motif (the RS cluster) and either a [2Fe−2S] cluster (BS)[7−9] or an additional [4Fe−4S] cluster (LS and MTTases) (the auxiliary cluster).[3,10−12] The RS cluster binds in contact with SAM and, in its reduced state ($[4Fe-4S]^+$), participates in the reductive fragmentation of SAM to a 5′-deoxyadenosyl 5′-radical (5′-dA·), a common intermediate among RS reactions.[6,13,14] The mechanistic details associated with sulfur insertion are not completely understood; however, it is believed that substrate radicals generated by abstraction of hydrogen atoms (H·) from target carbon centers by the 5′-dA· attack the bridging $\mu$-sulfido ions of the auxiliary clusters.[4,15] Because their auxiliary clusters are thought to be sacrificed during catalysis, RS enzymes that catalyze sulfur insertion typically catalyze no more than one turnover in vitro, although instances of higher product ratios have been reported.[3,16]

All known MTTases that act on tRNA modify adenosine 37 (A37), which resides immediately adjacent to the third nucleotide (position 36) of the anticodon. Before methylthiolation takes place, A37 must be modified at $N^6$ with either an isopentenyl or 4-hydroxyisopentenyl group (MiaB family) or a threonylcarbamoyl group (MtaB family). MiaA, a dimethylallyl pyrophosphate:tRNA dimethylallyltransferase, catalyzes the first committed step in the formation of $ms^2i^6A$, which is the transfer of an isopentenyl (dimethylallyl) group from dimethylallyl pyrophosphate (DMAPP) to $N^6$ of A37.[17−19] By contrast, four proteins (YgjD, YrdC, YjeE, and YeaZ) are required to generate the threonylcarbamoyl group at A37 of tRNAs that are modified by MtaB and its related proteins.[20,21] Hypermodifications of A37 are typically found on tRNAs that contain adenosine or uracil at position 36. Although

**Received:** May 14, 2013
**Published:** August 31, 2013

   dx.doi.org/10.1021/ja4048448 | *J. Am. Chem. Soc.* 2013, 135, 15404−15416

**Scheme 1. Reactions of the Three Major Classes of MTTases: (A) MiaB; (B) MtaB; (C) RimO[a]**

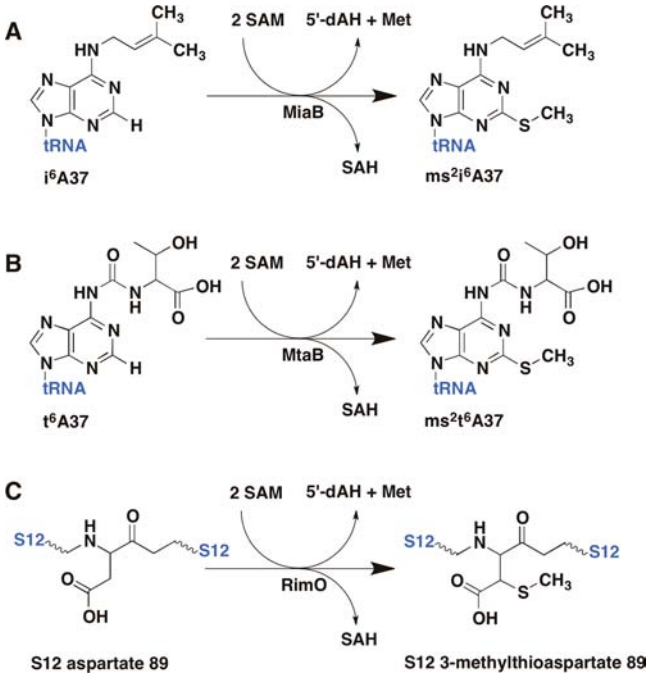


[a]In each reaction, two SAM molecules are cleaved to give one molecule of 5′-dA and one molecule of SAH.

nonessential,[22−24] they are believed to induce slight structural perturbations in the tRNA that permit increased exposure of the Watson−Crick faces of the anticodon to the RNA codon. This improved base pairing increases recognition of cognate tRNAs in the A-site over near-cognate tRNAs, thereby reducing ribosomal A-site pausing.[25] Moreover, improving the relatively weak adenosine−uridine pairing at the first base of the codon prevents ribosomal P-site slippage. The improvements in A-site and P-site recognition result in enhanced reading frame maintenance and therefore translational fidelity.[22−25] Recently, a member of the eukaryotic MtaB class of MTTases was shown to be one of the most reproducible genetic risk factors in the etiology of type-2 diabetes across multiple ethnic groups.[26−30]

RimO catalyzes methylthiolation of the $\beta$-carbon of aspartate 89 of protein S12 of the small subunit of the bacterial ribosome in *Ec* and a number of other bacteria, including *Thermotoga maritima* (*Tm*). The purpose of this modification is not yet known; it is neither universal nor essential for ribosome function. However, the inability to generate variants of D89 suggests that this residue, which projects toward the acceptor site of the ribosome, is essential and may play a role in some aspect of ribosome function.[31,32]

The MTTases represent a growing subclass of RS enzymes that use SAM as both a radical generator and a methyl donor. The best characterized members of this class are the RS methyltransferases/methylsynthases, which are represented by RlmN and Cfr.[33] These two proteins catalyze the synthesis of methyl groups on C2 and C8, respectively, of adenosine 2503 in 23*S* ribosomal RNA (rRNA),[34,35] employing a ping-pong-like mechanism of catalysis.[34] In the first half-reaction, SAM binds to the unique Fe ion of the sole [4Fe−4S] cluster in each protein and donates a methyl group to a conserved Cys residue, releasing *S*-adenosylhomocysteine (SAH) as the byproduct of the reaction.[34,36,37] In the second half-reaction, a second molecule of SAM binds to the same site but is reductively cleaved to a 5′-dA·, which initiates turnover by abstracting H· from the methyl-Cys residue. After radical addition to C2 or C8 of the adenine ring and loss of an electron to an undetermined acceptor, a methylene-bridged protein−substrate cross-link is resolved by disulfide bond formation with concomitant release of an enamine, which tautomerizes to the methyladenosine product upon acquiring a proton from a general acid in the active site.[34,38]

In this work, we show that *Tm* RimO and *Tm* MiaB also exhibit characteristics of a ping-pong-like reaction. Each protein catalyzes the formation of ∼1 equiv of SAH in the absence of substrate and reductant and an equal amount of methanethiol upon acid denaturation of the protein. Moreover, the introduction of methanethiol in assays conducted with *S*-adenosyl-L-[*methyl*-$d_3$]methionine ($d_3$-SAM) results in the formation of both unlabeled and deuterated products, showing that exogenous methanethiol can intercept the natural methylthiolating agent. Last, treatment of each protein with SAM in the absence of substrate or a low-potential reductant (i.e., dithionite) followed by treatment with $d_3$-SAM in the presence of substrate and dithionite results in a burst of unlabeled product followed by slower formation of the labeled product, suggesting that the radical-dependent transfer of a methylthio group to the substrate is fast relative to SAM-dependent methylation of the protein.

## MATERIALS AND METHODS

**Materials.** All of the DNA-modifying enzymes and reagents were obtained from New England Biolabs (Ipswich, MA), as was calf intestinal alkaline phosphatase. Nuclease P1 was obtained from US Biological. *Crotalus adamanteus* phosphodiesterase, sodium sulfide nonahydrate, L-tryptophan, 2-mercaptoethanol, L-(+)-arabinose, ferric chloride, sodium methanethiolate, 5′-deoxyadenosine (5′-dA), DMAPP, and SAH were purchased from Sigma (St. Louis, MO). *N*-(2-Hydroxyethyl)piperizine-*N*′-(2-ethanesulfonic acid) (HEPES) was purchased from Fisher Scientific (Pittsburgh, PA), and imidazole was purchased from J.T.Baker (Phillipsburg, NJ). Potassium chloride, glycerol, and the expression vectors pET-28a and pET-26b were purchased from EMD Chemicals (Gibbstown, NJ), while dithiothreitol (DTT) and nickel nitrilotriacetic acid (Ni-NTA) resin were purchased from Gold Biotechnology (St. Louis, MO). Coomassie blue dye-binding reagent for protein concentration determination was purchased from Pierce (Rockford, IL), as was the bovine serum albumin (BSA) standard (2 mg/mL). Nick, NAP-10, and PD-10 prepoured gel-filtration columns and Sephadex G-25 resin were purchased from GE Biosciences (Piscataway, NJ). All other buffers and chemicals were of the highest grade available.

**Preparation of Substrates for the *Tm* RimO, *Ec* MiaA, and *Tm* MiaB Reactions.** SAM, $d_3$-SAM, *S*-adenosyl-L-[*methyl*-$^{14}$C]-methionine ([*methyl*-$^{14}$C]SAM), and *S*-[8-$^{14}$C]adenosyl-L-methionine ([*adenosyl*-$^{14}$C]SAM) were synthesized and purified as described previously.[39] Oligonucleotide sequencing was conducted at the Penn State Huck Nucleic Acid Facility. The oligomeric ribonucleotide substrate for MiaB was synthesized by Dharmacon Thermo Fisher Scientific (Lafayette, CO). The RNA sequence corresponds to the 17-nucleotide anticodon stem−loop (ACSL) of *Ec* tRNA$^{Phe}$ (5′-GGGGAUUGAAAAUCCCC-3′). A37 (shown in bold type) is the site of modification by MiaA and MiaB. The S12 peptide substrate for RimO, $NH_2$-RGGRVK**D**LPGVRY-COOH (**1**), and a synthetic peptide substrate used as an external standard (ES), $NH_2$-PMSAPARSM-COOH (**2**), were synthesized by the Peptide Synthesis Facility at New England Biolabs as described previously[12] or by the Penn State Hershey College of Medicine Macro Core Facility. The sequence of peptide **1** corresponds to residues 83−95 of the *Ec* S12 protein, and the Asp residue in bold type (**D**) corresponds to D89, the site of methylthiolation.


dx.doi.org/10.1021/ja4048448 | J. Am. Chem. Soc. 2013, 135, 15404−15416

UV/vis spectra were recorded on a Cary 50 spectrometer from Varian (Walnut Creek, CA) using the WinUV software package for spectral manipulation and to control the instrument. Oxygen-sensitive samples were prepared in an anaerobic chamber and aliquoted into cuvettes that were sealed before being removed from the chamber. High-performance liquid chromatography (HPLC) was conducted on an 1100 system (Agilent Technologies, Santa Clara, CA) containing a variable-wavelength detector and an autosampler for sample injection. The instrument was operated via the ChemStation software package, which was also used for data analysis. Liquid chromatography/mass spectrometry (LC/MS) was conducted on an Agilent Technologies 1200 system coupled to an Agilent Technologies 6410 QQQ mass spectrometer with simultaneous UV/vis analysis using an Agilent diode-array detector. The system was operated with the associated MassHunter software package, which was also used for data collection and analysis. Sonic disruption of *Ec* cell suspensions was carried out as described previously,[12] and liquid scintillation counting was conducted on a Beckman LS 6500 scintillation counter using 5 mL of Ecoscint scintillation cocktail per milliliter of aqueous sample.

**Cloning and Overexpression of the *Tm miaB* and *Tm rimO* Genes.** The *Tm miaB* gene was amplified from *Tm* genomic DNA using polymerase chain reaction (PCR) technology. The forward amplification primer, 5′-CGC GGC GTC CAT ATG AGA TTT TAC ATA AAG ACC TTC GGC-3′, included an *Nde*I restriction site (underlined) flanked by a nine-base GC clamp and the first 27 bases of the *miaB* gene. The reverse primer, 5′-CGC GGC GTC GCG GCC GCC TCA GAA GAA GAA ACG GGA GAA GG-3′, contained a *Not*I restriction site (underlined) flanked by a nine-base GC clamp and the last 24 bases of the *miaB* gene, excluding the stop codon. The PCR was performed with a Robocycler thermocycler (Stratagene, La Jolla, CA) as described previously.[11] The product was isolated, digested with *Nde*I and *Not*I, and ligated into similarly digested pET-26b by standard procedures.[40] The correct construct, encoding a 5 amino acid (aa) linker between the gene product and a C-terminal hexahistidine tag, was verified by DNA sequencing and designated pTmMiaB.

The *Tm rimO* gene was similarly amplified from *Tm* genomic DNA using the forward primer 5′-CGC GGC GTC CAT ATG AGG GTT GGT ATA AAG GTT CTA GGA TGT CC-3′ and the reverse primer 5′-CGC GGC GTC GAA TTC TCA TAT CAC TGA CCC CCA CAT GTC GTA CTC G-3′. The forward primer included an *Nde*I restriction site (underlined) flanked by a nine-base GC clamp and the first 29 bases of the *rimO* gene. The reverse primer contained an *Eco*RI restriction site (underlined) flanked by a nine-base GC clamp and the last 31 bases of the *rimO* gene, including the stop codon. After amplification, the product was digested with *Nde*I and *Eco*RI and ligated into similarly digested pET-28a by standard procedures. The correct construct was verified by DNA sequencing and designated pTmRimO.

The expression vectors pTmMiaB and pTmRimO were transformed into *Ec* BL21(DE3) along with plasmid pDB1282 as previously described.[41,42] Bacterial growth and gene expression were carried out at 37 °C in 16 L of M9 minimal medium distributed evenly among four Erlenmeyer flasks with moderate shaking (180 rpm). At an optical density at 600 nm ($OD_{600}$) of 0.3, solid L-(+)-arabinose was added to each flask to a final concentration of 0.2% (w/v), while cysteine and ferric chloride were added to final concentrations of 300 and 50 $\mu$M, respectively. At an $OD_{600}$ of 0.6, a sterile solution of isopropyl-$\beta$-D-thiogalactopyranoside (IPTG) was added to each flask to a final concentration of 200 $\mu$M. Expression was allowed to take place for 16 h at 18 °C before the cells were harvested by centrifugation at 10000*g* for 10 min at ambient temperature.

**Purification of *Tm* MiaB and *Tm* RimO.** Purification of *Tm* MiaB and *Tm* RimO was carried out by immobilized metal affinity chromatography (IMAC) using Ni-NTA resin. Unless specifically stated otherwise, all purification steps were performed in a anaerobic chamber (Coy, Grass Lakes, MI) that was kept under an atmosphere of $N_2$ and $H_2$ (95%/5%). The $O_2$ concentration was maintained below 1 ppm by using palladium catalysts. Buffers used during the purification of *Tm* RimO were as follows: lysis buffer (50 mM HEPES, pH 7.5, 300 mM KCl, 10 mM 2-mercaptoethanol, 20 mM imidazole, and 1 mg/mL lysozyme); wash buffer (50 mM HEPES, pH 7.5, 300 mM KCl, 10 mM 2-mercaptoethanol, 10% (v/v) glycerol, and 40 mM imidazole); elution buffer (wash buffer containing 250 mM imidazole). Buffers used during the purification of *Tm* MiaB were similar. After the cells were lysed by sonication,[41] the cell suspension was transferred into sterile centrifuge tubes, which were subsequently sealed and heated at 70 °C for 1 h (RimO) or at 75 °C for 15 min (MiaB) outside of the anaerobic chamber. After the heat-treated solution was subjected to centrifugation at 50000*g* and ambient temperature for 1.5 h, the supernatant was loaded onto a Ni-NTA column, which was subsequently washed with an appropriate volume of wash buffer. After addition of elution buffer to the column, fractions containing MiaB or RimO, distinguished by their dark-brown color, were pooled and concentrated using an Amicon stirred ultrafiltration apparatus (Millipore, Billerica, MA) fitted with a YM-30 membrane (30 000 molecular weight cutoff). The protein was exchanged into gel-filtration buffer (GFB) (50 mM HEPES, pH 7.5, 300 mM KCl, 20% glycerol, and 1 mM DTT) using a Sephadex G-25 column (2.5 cm × 13 cm), reconcentrated, and stored in aliquots in a liquid $N_2$ dewar until ready for use.

**Cloning and Overexpression of the *Ec miaA* Gene and Purification of MiaA.** The *miaA* gene was amplified from *Ec* genomic DNA using PCR technology. The forward amplification primer, 5′-CGC GGC GTC CAT ATG AGT GAT ATC AGT AAG GCG AGC CTG CCT-3′, included an *Nde*I restriction site (underlined) flanked by a nine-base GC clamp and the first 30 bases of the *miaA* gene, including the start codon. The reverse primer, 5′-CGC GGC GTC CTC GAG TCA GCC TGC GAT AGC ACC AAC AAC CTG-3′, contained a *Xho*I restriction site (underlined) flanked by a nine-base GC clamp and the last 27 bases of the *miaA* gene, including the stop codon. The PCR was performed as described previously,[11] and the product was isolated, digested with *Nde*I and *Xho*I, and ligated into similarly digested pET-28a by standard procedures. The correct construct, also encoding an N-terminal hexahistidine tag and 10 aa linker, was verified by DNA sequencing and designated pEcMiaA. pEcMiaA was transformed into *Ec* BL21(DE3) for gene expression.

Bacterial growth and gene expression were carried out at 37 °C in 16 L of Luria−Bertani medium evenly distributed in four Erlenmeyer flasks. The flasks were subjected to moderate shaking (180 rpm) throughout the procedure. At an $OD_{600}$ of 0.6, a sterile solution of IPTG was added to each flask to a final concentration of 200 $\mu$M. Expression was allowed to take place for 4 h at 37 °C before the cells were harvested by centrifugation at 10000*g* for 10 min at ambient temperature.

MiaA was purified by IMAC as described above using the following buffers: lysis buffer (50 mM HEPES, pH 7.5, 300 mM KCl, 10 mM imidazole, and 1 mg/mL lysozyme); wash buffer (50 mM HEPES, pH 7.5, 300 mM KCl, and 20 mM imidazole); elution buffer (50 mM HEPES, pH 7.5, 300 mM KCl, 250 mM imidazole, and 10 mM 2-mercaptoethanol). After sonic disruption of the cells, the crude lysate was subjected to centrifugation at 50000*g* for 1.5 h. The supernatant was loaded onto Ni-NTA resin, which was subsequently washed with an appropriate volume of wash buffer and then eluted with elution buffer. Fractions displaying absorbances at 280 nm were pooled and concentrated using an Amicon stirred ultrafiltration apparatus. MiaA was exchanged into 50 mM HEPES, pH 7.5, 300 mM KCl, and 20% glycerol using a Sephadex G-25 column and then reconcentrated, snap-frozen, and stored in small aliquots at −80 °C.

**Protein, Iron, and Sulfide Quantification.** The concentrations of *Tm* RimO and *Tm* MiaB were determined by the procedure of Bradford[43] using BSA (fraction V) as a standard. Quantitative amino acid analysis, conducted as described previously,[44] indicated that the procedure of Bradford overestimated the concentrations of *Tm* RimO and *Tm* MiaB by factors of 1.47 and 1.53, respectively. Iron and sulfide analyses were performed according to the procedures of Beinert.[45−47]

**Chemical Reconstitution of *Tm* RimO and *Tm* MiaB.** *Tm* RimO and *Tm* MiaB were treated with 10 mM DTT before being incubated for 10 min with an 8-fold molar excess of $FeCl_3$. An 8-fold molar excess of sodium sulfide was added over the course of 3−4 h, upon which the solution was subjected to centrifugation at 18000*g*.


dx.doi.org/10.1021/ja4048448 | J. Am. Chem. Soc. 2013, 135, 15404−15416

The supernatant was exchanged into storage buffer by gel-filtration (G-25) chromatography and concentrated by ultrafiltration using an Amicon stirred ultrafiltration apparatus fitted with a YM-10 membrane. Following chemical reconstitution, *Tm* RimO and *Tm* MiaB were further purified by fast protein liquid chromatography (FPLC) on an S-200 column using an ÄKTA liquid chromatography system (GE Biosciences) housed in an anaerobic chamber. The column was equilibrated in buffer consisting of 10 mM HEPES, pH 7.5, 500 mM KCl (150 mM for MiaB), 5 mM DTT (1 mM for MiaB), and 10% glycerol. Fractions were pooled on the basis of their absorbances at 280 and 400 nm and concentrated and stored as described above.

**MiaB Activity Assays.** The 17-nucleotide ACSL RNA substrate was denatured by heating at 75 °C for 5 min and then quickly cooled on ice to generate the appropriate hairpin secondary structure. Isopentenylation of the ACSL RNA was carried out by incubating 100 $\mu$M ACSL RNA, 300 $\mu$M DMAPP, 50 mM Tris-HCl, pH 7.5, 3.5 mM $MgCl_2$, 5 mM 2-mercaptoethanol, and 5 $\mu$M *Ec* MiaA for 1 h at 37 °C.[48] The reaction was terminated by heating at 60 °C for 10 min, and the reaction mixture was subjected to centrifugation. The supernatant was removed, and the RNA was exchanged into 10 mM Tris-HCl, pH 6.5, and 10% glycerol by anaerobic gel-filtration chromatography (AGFC) using Sephadex G-25 resin. The resulting concentration of the ACSL RNA was determined from its UV/vis absorbance using a theoretical extinction coefficient ($\varepsilon_{260}$ = 170 500 $M^{-1}$ $cm^{-1}$) supplied by Dharmacon Thermo Fisher Scientific. The ACSL RNA was determined to be completely modified by MiaA, with each mole of RNA containing 1 mol of $i^6A$. Quantification was conducted by LC/MS using a standard curve generated from commercially available $i^6A$ (Sigma). The RNA was snap-frozen and stored in small aliquots in a liquid $N_2$ dewar.

MiaB assays contained the following in a volume of 330 $\mu$L: 100 $\mu$M reconstituted (RCN) MiaB, 200 $\mu$M $i^6A$ ACSL RNA substrate, 500 $\mu$M SAM, 50 mM Tris-HCl, pH 7.5, 1 mM dithionite, and 686 $\mu$M tryptophan as an internal standard (IS). All components except SAM were incubated for 3 min at 37 °C before the reaction was initiated with SAM. At designated times, 30 $\mu$L aliquots of the reaction were removed and added to 30 $\mu$L of 0.2 M $H_2SO_4$. A portion of the quenched samples was removed for quantification of 5′-dA and SAH, while the remaining volume was titrated to pH 5−6 with Tris-HCl, pH 8.0, before digestion of the RNA sequentially with nuclease P1,[49] *C. adamanteus* phosphodiesterase, and calf-intestinal alkaline phosphatase by referenced procedures.[50] The resulting precipitate was pelleted by centrifugation, and the supernatants were lyophilized to dryness in vacuo and redissolved in an appropriate volume of $H_2O$.

Samples to be analyzed by LC/MS were injected onto an Agilent Zorbax Rapid Resolution XDB-C18 column (4.6 mm × 50 mm × 1.8 $\mu$m particle size) equilibrated in 98% solvent A (40 mM ammonium acetate, pH 6.2) and 2% solvent B (acetonitrile). The following gradient was applied: 2% solvent B (0.5 min), 2−12% solvent B (4 min), 12−24% solvent B (1.5 min), 24−50% solvent B (1 min), 50% solvent B (4.5 min), 50−2% solvent B (1 min). The column was equilibrated with 2% solvent B for 2.5 min between sample injections. Products were detected in positive-ion mode using the neutral loss of the ribose ring ($m/z$ 132.1). The $i^6A$ substrate (8.2 min) and $ms^2i^6A$ product (8.9 min) were detected at $m/z$ 336.2 [M + 1] and 382.2 [M + 1], respectively, while SAH (2.8 min) and 5′-dA (5.3 min) were detected at $m/z$ 385.1 and 252.1, respectively. In most instances, the kinetic data were fit to a first-order single-exponential equation to extract the amplitude ($A$) and rate constant ($k$). The initial rate ($v$) was then estimated as the product of the amplitude and rate constant for the given curve.

**Generation of an $ms^2i^6A$ Standard.** The $ms^2i^6A$ RNA standard was generated by reacting the $i^6A$ ACSL RNA with MiaB under turnover conditions. Reactions contained the following in a final volume of 180 $\mu$L: 350 $\mu$M $i^6A$ ACSL RNA, 400 $\mu$M MiaB, 1 mM SAM, and 1 mM dithionite. The reactions were initiated by the addition of MiaB, and the reaction mixtures were incubated at 37 °C for 3 h. Samples were diluted to 300 $\mu$L with $ddH_2O$ and then adjusted to 50 mM NaOH (final concentration) before being extracted with an equal volume of phenol/chloroform/isoamyl alcohol (25:24:1). The RNA was then precipitated with ethanol by standard procedures. After centrifugation, the RNA precipitate was dissolved in 10 mM HEPES, pH 6.5, with 10% glycerol (v/v) and quantified spectrophotometrically ($\varepsilon_{260}$ = 170 500 $M^{-1}$ $cm^{-1}$). Verification of full conversion of the $i^6A$ ACSL RNA to the desired $ms^2i^6A$ product was accomplished by LC/MS after RNA digestion as described above. Standard curves were prepared using dilutions of this $ms^2i^6A$ RNA product in 50 mM Tris-HCl, pH 7.5, assuming 1 mol of $ms^2i^6A$ per mole of ACSL RNA strand. Each sample in the standard curve was treated exactly as each assay time point.

***Tm* RimO Activity Assays.** *Tm* RimO reactions contained the following in a final volume of 180 $\mu$L: 67 $\mu$M *Tm* RimO, 700 $\mu$M SAM, 300 $\mu$M S12 peptide substrate **1**, 50 mM Na-HEPES, pH 7.5, 2 mM dithionite, and 1 mM tryptophan (IS). All components except SAM were incubated at 37 °C for 3 min before the reaction was initiated with the omitted component. Aliquots (20 $\mu$L) of the reaction mixture were withdrawn at various times from 0 to 180 min and added to 20 $\mu$L of 0.1 M $H_2SO_4$ containing 20 $\mu$M peptide **2** (ES) to quench the reaction. Precipitated protein was removed by centrifugation at 18000*g* for 15 min, and a 20 $\mu$L aliquot of the resulting supernatant was subjected to analysis by positive-ion-mode electrospray ionization LC/MS with single-ion monitoring (SIM). Solvent A consisted of ammonium acetate (40 mM) and methanol (5% v/v) titrated to pH 6.2 with acetic acid, while solvent B was 100% acetonitrile. The column was equilibrated in 100% solvent A at a flow rate of 0.5 mL $min^{-1}$. After sample injection (2 $\mu$L), the following gradient was applied: 0−2% solvent B (0.5 min), 2−28% solvent B (4.5 min), 50−2% solvent B (3 min). The monitored ions ($m/z$) and retention times (min), respectively, were 385.1 and 0.8 for SAH, 188.0 and 1.2 for tryptophan, 252.1 and 2.1 for 5′-dA, 474.4 and 3.2 for peptide **2** (ES), 498.1 and 4.4 (peptide **1**), and 507.1 and 4.4 for methylthiolated **1** (MS-**1**). Calibration curves were generated with known concentrations of each analyte and run under identical conditions to determine the concentrations of products generated in the assays. Data were analyzed using the Agilent Technologies MassHunter qualitative and quantitative analysis software. In most instances, the kinetic data were fit to a first-order single-exponential equation to extract the amplitude ($A$) and the rate constant ($k$). The initial rate ($v$) was then estimated as the product of the amplitude and rate constant for the given curve.

***Tm* RimO and *Tm* MiaB Radioactivity Assays.** *Tm* RimO was incubated for 1−2 h at 37 °C with [*methyl*-$^{14}$C]SAM (specific radioactivity: 910 cpm/nmol) or [*adenosyl*-$^{14}$C]SAM (specific radioactivity: 1110 cpm/nmol) in reactions containing the following in a total volume of 100 $\mu$L: 50 mM HEPES, pH 7.5, 273 $\mu$M *Tm* RimO, and 1 mM radiolabeled SAM. After incubation, the reaction mixtures were applied to prepoured gel-filtration columns equilibrated in (i) 10 mM HEPES, pH 7.5, 150 mM KCl, 10% glycerol, and 5 mM DTT; (ii) 10 mM HEPES, pH 7.5, 150 mM KCl, 10% glycerol, 5 mM DTT, and 200 mM NaOH; or (iii) 10 mM HEPES, pH 7.5, 150 mM KCl, 10% glycerol, 5 mM DTT, and 8 M urea. A 200 $\mu$L aliquot of the protein-containing fraction (400 $\mu$L total volume) was analyzed directly by scintillation counting. A 50 $\mu$L aliquot of the protein-containing fraction was added to 10 $\mu$L of a carrier solution containing 100 $\mu$M each of SAM, SAH, 5′-dA, adenine, and methylthioadenosine (MTA). The resulting solution was acidified by addition of 60 $\mu$L of 100 mM $H_2SO_4$ before a 100 $\mu$L aliquot was withdrawn for HPLC analysis as described above for detection of 5′-dA and SAH. Fractions were collected throughout the entire chromatographic procedure, and fractions with retention times corresponding to those of each carrier component were pooled and subjected to scintillation counting. Control samples containing either of the two radiolabeled forms of SAM but lacking *Tm* RimO were prepared and treated as described above for the complete assays. *Tm* MiaB was treated in the same fashion except that the initial incubation reaction with [*methyl*-$^{14}$C]-SAM or [*adenosyl*-$^{14}$C]SAM contained the following components: 200 $\mu$M MiaB, 886 $\mu$M radiolabeled SAM, and 50 mM HEPES, pH 7.5.

**Determination of *Tm* RimO- and *Tm* MiaB-Dependent Production of Methanethiol.** Assays contained the following

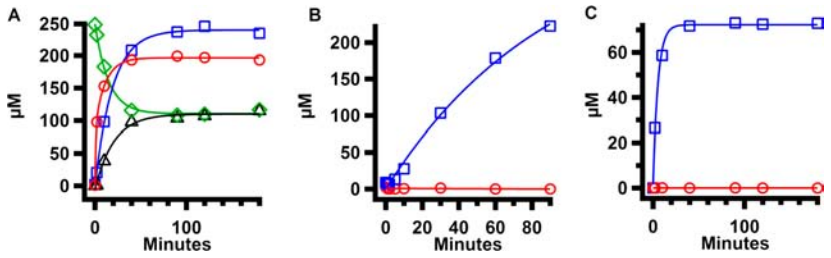


**Figure 1.** *Tm* RimO-catalyzed reactions at 37 °C (A) under turnover conditions with SAM, **1**, and dithionite; (B) in the presence of SAM and dithionite but the absence of **1**, and (C) in the presence of SAM but the absence of dithionite and **1**. SAH formation (blue squares), 5′-dA formation (red circles), MS-**1** formation (black triangles), consumption of **1** (green diamonds). The reactions were conducted as described in Materials and Methods, and contained, where appropriate, 67 μM *Tm* RimO, 300 μM **1**, 1 mM SAM, and 2 mM dithionite. The lines are fits to a first-order single-exponential equation with the following kinetic parameters: (A) SAH formation: $A = 239 \pm 3$ μM, $v = 11.9 \pm 0.7$ μM min$^{-1}$; 5′-dA formation: $A = 183 \pm 17$ μM, $v = 47.6 \pm 4.4$ μM min$^{-1}$; MS-**1** formation: $A = 115 \pm 6$ μM, $v = 5.8 \pm 0.3$ μM min$^{-1}$; consumption of **1**: $A = 139 \pm 4$ μM, $v = 9.7 \pm 0.3$ μM min$^{-1}$ (B) SAH formation: $A = 359 \pm 65$ μM, $v = 3.6 \pm 0.7$ μM min$^{-1}$; (C) SAH formation: $A = 72 \pm 1$ μM, $v = 13.7 \pm 0.2$ μM min$^{-1}$, $k = 0.19 \pm 0.02$ min$^{-1}$.

components in a final volume of 700 μL: 50 mM HEPES, pH 7.5, 1 mM SAM, 1 mM tryptophan, 67 μM *Tm* RimO or 100 μM *Tm* MiaB, 1 mM SAM, and, when appropriate, 300 μM S12 peptide or 200 μM i$^6$A ACSL RNA. Reactions were performed in triplicate at ambient temperature in septum-sealed vials and were initiated by addition of SAM. At designated times, 20 μL aliquots were removed and added to equal volumes of 0.1 M $H_2SO_4$ for quantification of SAH by LC/MS. An equal volume of 1 M HCl was injected into the remaining 80 μL, and the reaction was incubated further at 42 °C for 30 min to allow equilibration of methanethiol between the liquid and gas phases. An aliquot (500 μL) of the headspace was removed using a gastight syringe and analyzed by gas chromatography/mass spectrometry (GC/MS) using a Shimadzu GC-17A gas chromatograph connected to a Shimadzu GCMS-QP500 mass spectrometer and a Restek Rxi-1 ms 30 m column (i.d., 0.32 narrow bore; film, 4.0 μm) (Restek, Bellefonte, PA). The inlet and oven temperatures were both maintained at 30 °C, while the detector was set to 300 °C. Total ion chromatograms were generated under SIM conditions ($m/z$ 47).

***Tm* RimO Differential Labeling Assays.** A reaction mixture containing 533 μM *Tm* RimO, 50 mM Na-HEPES, pH 7.5, and 1 mM SAM in a total volume of 100 μL was incubated for 18 h at 37 °C and then subjected to AGFC to remove SAH and unreacted SAM. After the concentration of *Tm* RimO was determined following AGFC (132 μM), the protein (66 μM) was incubated with 0.7 mM [*methyl*-$d_3$]SAM for 3 min, 1 h, or 3 h before turnover was initiated by addition of dithionite. At appropriate times, aliquots of the reaction mixture were removed, and the reaction was quenched with an equal volume of 0.1 M $H_2SO_4$ containing peptide **2** (**ES**). The resulting mixtures were then analyzed for SAH, 5′-dA, and labeled and unlabeled MS-**1** by LC/MS.

***Tm* MiaB Differential Labeling Assays.** Assays contained 150 μM RCN *Tm* MiaB, 50 mM Tris-HCl, pH 7.5, and 686 μM tryptophan (IS) in a volume of 180 μL. Reactions were conducted over a period of 2 h at 37 °C and were initiated by addition of 150 μM (final concentration) SAM. At appropriate times, 10 μL aliquots were removed and added to 10 μL of 0.2 M $H_2SO_4$ to quench the reaction, and the resulting samples were analyzed by HPLC to determine the extent of SAH formation as described above. Afterward, $d_3$-SAM (500 μM final concentration) and *Ec* i$^6$A ACSL substrate (130 μM final concentration) were added to the remaining volume of unquenched reaction mixture containing 100 μM (final concentration) *Tm* MiaB, and turnover was initiated by addition of 1 mM dithionite after preincubation at 37 °C for 3 min. At indicated times over a 2 h period, 10 μL aliquots were removed and added to 10 μL of 0.2 M $H_2SO_4$ to quench the reaction. Aliquots (10 μL) of the quenched samples were analyzed by HPLC for 5′-dA and SAH, while the remaining volumes were analyzed for ms$^2$i$^6$A by LC/MS as described above.

## RESULTS

In our previous studies of *Ec* RimO, we reported that the enzyme catalyzed the formation of SAH in the absence of dithionite and substrate.[12] This behavior was also observed in our studies of the methyltransferases/methylsynthases Cfr and RlmN, which are the best characterized of the RS enzymes that use SAM as both a precursor to 5′-dA· to initiate radical-dependent chemistry and the source of an appended methyl group.[37] This observation suggested the possibility that, similar to RlmN and Cfr, the MTTases might also operate via a ping-pong mechanism wherein the methyl group is first appended to an amino acid residue or enzyme prosthetic group before being transferred to the product. Although the amount of turnover by *Ec* RimO was exceedingly low, SAH was generated in amounts similar to those of the methylthiolated product.[12] Similar studies by Arragain and co-workers on *Tm* RimO showed that this enzyme is better suited for mechanistic interrogation, as it supported production of ∼2 nmol of product per nanomole of RimO polypeptide.[3] Interestingly, the authors reported that *Tm* RimO catalyzed the production of the intended monomethylthiolated product as well as a bismethylthiolated product when a 20 aa peptide containing the sequence surrounding D89 of protein S12 was used as a substrate. The former product was shown to contain the methylthiol modification at the intended location (D89), but the location of the second methylthiol group was not determined. The authors also reported that SAH was produced in a reaction mixture lacking the peptide substrate but requiring dithionite, but they did not provide supporting data.[3,16]

To determine whether methyl transfer in the absence of substrate and dithionite is a general characteristic of MTTases, we cloned genes that encode both RimO and MiaB from *Tm* to study the behavior of their encoded proteins. Both the *Tm rimO* and *Tm miaB* genes were coexpressed with genes on plasmid pDB1282, which encodes proteins involved in Fe/S cluster biosynthesis and insertion in *Azotobacter vinelandii*.[42,51] *Tm* RimO was produced with an N-terminal hexahistidine tag, while *Tm* MiaB was produced with a C-terminal hexahistidine tag. Both proteins were routinely reconstituted with additional iron and sulfide using previously described methods.[12,42] Displayed in Figure S1 in the Supporting Information are typical UV−vis traces of as-isolated (AI) and RCN *Tm* RimO (solid and dashed lines, respectively, in Figure S1A) and AI and RCN *Tm* MiaB (solid and dashed lines, respectively, in Figure S1B), which are similar to those reported previously.[3,10,12]


dx.doi.org/10.1021/ja4048448 | J. Am. Chem. Soc. 2013, 135, 15404−15416

**Turnover by *Tm* RimO.** Turnover by *Tm* RimO was measured using a 13 aa synthetic peptide composed of the sequence surrounding D89 (bold type) of protein S12, $NH_2$-RGGRVK**D**LPGVRY-COOH (**1**), which is perfectly conserved between *Ec* and *Tm*. Quantification of SAM, SAH, 5′-dA, and S12 peptide **1** was conducted by LC/MS using standard curves that were constructed with authentic compounds. The methylthiolated peptide MS-**1** was quantified using **1** with the assumption that it ionized with similar efficiency. Consistent with this assumption, the time-dependent concentrations of MS-**1** formation and **1** decay were similar within the error associated with the method, and no other peptide-related species were observed during analysis (Figure 1A). The S12 peptide exhibited an ion at $m/z$ 491.8 (+3 charge state), and MS-**1** exhibited an ion at $m/z$ 507.1 (+3 charge state). No evidence of a peak at $m/z$ 522.4 (+3 charge state), which would correspond to a bismethylthiolated species, was observed. The bismethylthiolated species was also unobserved when the +1 or +2 charge states were monitored. Figure 1A depicts the time-dependent formation of MS-**1** (black line), 5′-dA (red line), and SAH (blue line) under turnover conditions in the presence of 67 $\mu$M *Tm* RimO as well as the time-dependent loss of **1** (green line). In contrast to our previous studies on *Ec* RimO, wherein the amount of SAH generated was meager (<10% of the concentration of enzyme), *Tm* RimO catalyzed the formation of ∼3 equiv of 5′-dA and 4 equiv of SAH per equivalent of enzyme in ∼80 min. Importantly, the concentration of MS-**1** formed (∼114 $\mu$M) was nearly twice the *Tm* RimO concentration in the assay (67 $\mu$M) as was the concentration of peptide consumed (∼131 $\mu$M), and the initial rate for MS-**1** formation (5.8 ± 0.3 $\mu$M $min^{-1}$) was similar (within error) to the initial rate of consumption of **1** (9.7 ± 0.3 $\mu$M $min^{-1}$). Therefore, it appears that *Tm* RimO catalyzes more than one turnover, as shown previously.[3,16] Figure 1B depicts a *Tm* RimO reaction containing SAM and dithionite but lacking **1**. SAH was still produced at a similar concentration after 80 min of reaction; however, time-dependent formation of 5′-dA (red line) and MS-**1** was not observed, implying that the peptide substrate triggers radical generation but not SAH formation. Interestingly, SAH was generated relatively rapidly ($v$ = 13.7 ± 0.2 $\mu$M $min^{-1}$), but in a 3-fold lower concentration when both dithionite and **1** were omitted (Figure 1C). Moreover, the concentration of SAH generated (73 $\mu$M) was almost equivalent to the concentration of enzyme in the assay (67 $\mu$M). This behavior implies that *Tm* RimO does not require that radical chemistry take place before methyl transfer, presenting the possibility that sulfur insertion may not precede methyl transfer as had been suggested previously.[1]

To determine the nature of the species to which SAM donates its methyl moiety in the absence of substrate and/or reductant, studies were conducted with [*methyl*-$^{14}$C]SAM or [*adenosyl*-$^{14}$C]SAM (Figure 2). When *Tm* RimO (43.1 nmol) was incubated with [*methyl*-$^{14}$C]SAM to allow for methyl transfer and then the reaction mixture was subjected to AGFC, two peaks of radioactivity were observed, an early peak containing the protein fraction and a later peak containing only small molecules (Figure 2B). From the specific radioactivity of SAM, it was calculated that 33.4 nmol (∼0.75 equiv) of radioactivity was attached to the protein (Figure 2B). A control experiment in which an equal concentration and amount of [*methyl*-$^{14}$C]SAM was applied to the gel-filtration column in the absence of *Tm* RimO showed the presence of only one peak of radioactivity, which eluted with the small

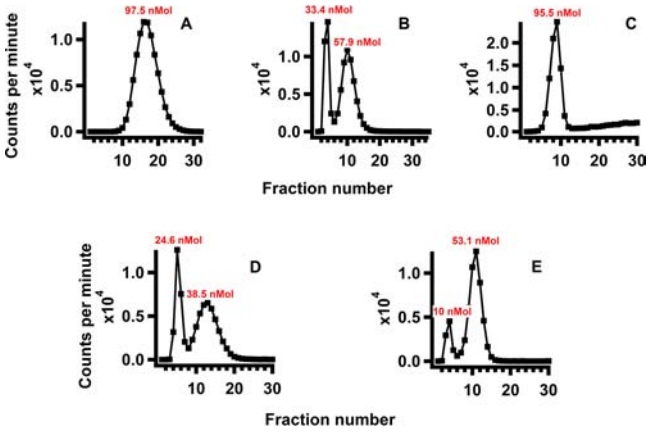


**Figure 2.** Elution profiles of *Tm* RimO incubated with [*methyl*-$^{14}$C]-SAM or [*adenosyl*-$^{14}$C]SAM and analyzed subsequent to anaerobic gel-filtration chromatography (AGFC) under various conditions: (A) [*methyl*-$^{14}$C]SAM in gel-filtration buffer (GFB); (B) *Tm* RimO + [*methyl*-$^{14}$C]SAM in GFB; (C) *Tm* RimO + [*methyl*-$^{14}$C]SAM in GFB + 200 mM NaOH; (D) *Tm* RimO + [*adenosyl*-$^{14}$C]SAM; (E) *Tm* RimO + [*methyl*-$^{14}$C]SAM in GFB containing 8 M urea.

molecules (Figure 2A). As shown in Figure 2C, when *Tm* RimO was incubated with excess [*methyl*-$^{14}$C]SAM and mixture was then applied to a gel-filtration column equilibrated in GFB containing 0.2 N NaOH, no radioactivity eluted with the protein fraction, consistent with attachment of the radioactive moiety to a species that is unstable under very basic conditions. In a similar experiment in which the reaction mixture was applied to a gel-filtration column equilibrated in GFB containing 8 M urea, only 10 nmol of radioactivity eluted with the protein fraction (Figure 2E), suggesting that the stability of the methyl acceptor is influenced by the integrity of the overall fold of the protein.

In a subsequent experiment, *Tm* RimO was incubated for 2 h at 37 °C with [*methyl*-$^{14}$C]SAM in the absence of substrate and dithionite and then subjected to AGFC. The protein fraction (6.8 nmol) was treated with 50 mM $H_2SO_4$ (final concentration), and a fraction of the resulting supernatant obtained after centrifugation was analyzed by HPLC with radiometric detection. As shown in Figure S2B in the Supporting Information, very little radioactivity in SAM (0.2 nmol), 5′-dA (0.003 nmol), SAH (0.003 nmol), adenine (0.29 nmol), or MTA (0.002 nmol) eluted with the protein after AGFC, and no other significant peaks of radioactivity were found in any other region of the chromatogram. Experiments conducted with [*adenosyl*-$^{14}$C]SAM corroborated the observations obtained using [*methyl*-$^{14}$C]SAM. When *Tm* RimO (43.1 nmol) was incubated with excess [*adenosyl*-$^{14}$C]SAM and then subjected to AGFC, ∼24.6 nmol of radioactivity eluted with the protein fraction (Figure 2D). Upon analysis of a portion of the protein-containing fraction by HPLC with radiometric detection, the vast majority of the radioactivity (2.8 nmol) eluted with the SAH standard (Figure S2A), while only 0.23 nmol eluted with SAM. These observations suggest that upon binding of SAM to *Tm* RimO, transfer of a methyl group from SAM to an acid- and base-labile acceptor takes place. Moreover, the labile acceptor appears to be volatile under acidic conditions, as the radiolabeled methyl group was not observed during HPLC with radiometric detection. The instability of the methylated species in the presence of urea argues that the methyl group is not transferred to an amino acid (e.g., Glu or


dx.doi.org/10.1021/ja4048448 | J. Am. Chem. Soc. 2013, 135, 15404−15416

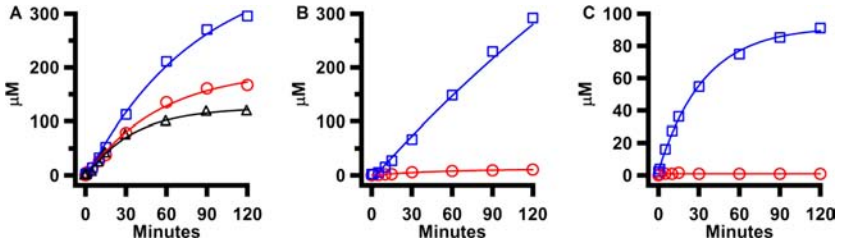


**Figure 3.** *Tm* MiaB-catalyzed reactions at 37 °C showing the generation of 5′-dA (red circles), SAH (blue squares) and $ms^2i^6A$ (black triangles): (A) under turnover conditions with SAM, $i^6A$ ACSL tRNA, and dithionite; (B) in the presence of SAM and dithionite but the absence of $i^6A$ ACSL tRNA; (C) in the presence of SAM but the absence of dithionite and $i^6A$ ACSL tRNA. The reactions were conducted as described in Materials and Methods and contained, where appropriate, 100 $\mu$M *Tm* MiaB, 200 $\mu$M $i^6A$ ACSL tRNA, 500 $\mu$M SAM, and 1 mM dithionite. Lines are fits to a first-order single-exponential equation with the following parameters: (A) 5′-dA formation: $A = 195 \pm 12$ $\mu$M, $v = 3.5 \pm 0.6$ $\mu$M $min^{-1}$; SAH formation: $A = 397 \pm 36$ $\mu$M, $v = 4.8 \pm 1.2$ $\mu$M $min^{-1}$; $ms^2i^6A$ formation: $A = 125 \pm 4$ $\mu$M, $v = 3.6 \pm 0.5$ $\mu$M $min^{-1}$; (B) SAH formation: rate $= 2.5 \pm 0.1$ $\mu$M $min^{-1}$ (linear fit); (C) SAH formation: $A = 92 \pm 1$ $\mu$M, $v = 2.8 \pm 0.2$ $\mu$M $min^{-1}$.

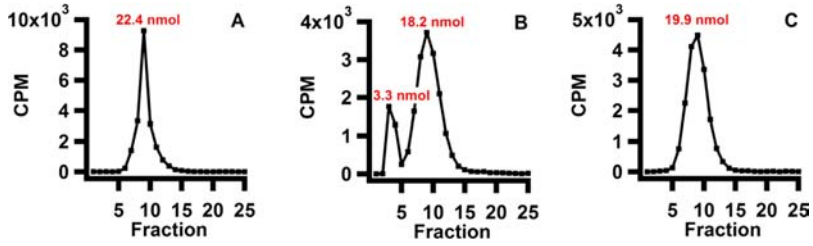


**Figure 4.** Elution profiles of *Tm* MiaB incubated with [*methyl*-$^{14}$C]SAM and analyzed subsequent to AGFC under various conditions: (A) [*methyl*-$^{14}$C]SAM in GFB; (B) *Tm* MiaB + [*methyl*-$^{14}$C]SAM in GFB; (C) *Tm* MiaB + [*methyl*-$^{14}$C]SAM in GFB + 200 mM NaOH.

Asp) to afford an ester or some other acid- or base-labile organic species but rather to an acceptor whose presence depends on the integrity of the overall protein fold.

**Turnover by *Tm* MiaB.** Similar results were obtained with *Tm* MiaB, suggesting that the above behavior may be a general trait of MTTases and therefore mechanistically relevant. Although the natural substrates for MiaB are specific full-length tRNAs, studies by Pierrel et al.[52] showed that a 17-base oligonucleotide corresponding to the ACSL region of *Ec* $tRNA^{Phe}$ is also efficiently modified. This substrate was obtained commercially and then isopentenylated using MiaA.[52,53] Figure 3 depicts the time-dependent formation of $ms^2i^6A$, 5′-dA, and SAH with *Tm* MiaB under various conditions. All of the products save $ms^2i^6A$ were quantified by LC/MS using commercially available standards. A 17-base oligonucleotide standard containing $ms^2i^6A$ at the appropriate position was used for accurate quantification of $ms^2i^6A$. This standard was generated enzymatically in large-scale MiaA and MiaB reactions using the commercially available 17-base ACSL of *Ec* $tRNA^{Phe}$. Under turnover conditions in reactions initiated by addition of SAM, 100 $\mu$M *Tm* MiaB catalyzed the formation of ~115 $\mu$M (~1.2 equiv) $ms^2i^6A$ (Figure 3A, black trace), 150 $\mu$M 5′-dA (Figure 3A, red trace), and 300 $\mu$M SAH (Figure 3A, blue trace) after 2 h at 37 °C. When the 17-base ACSL tRNA was omitted from the reaction mixture, the formation of 5′-dA was arrested (Figure 3B, red trace), but the formation of SAH still occurred to a similar extent after a 2 h incubation (Figure 3B, blue trace). Similar to the behavior of *Tm* RimO, in the absence of both dithionite and substrate, *Tm* MiaB catalyzed the formation of ~90 $\mu$M (0.9 equiv) SAH (Figure 3C, blue trace) with an initial rate of $2.8 \pm 0.2$ $\mu$M $min^{-1}$. Again, this behavior suggests that *Tm* MiaB does not require radical chemistry to take place before methyl transfer, presenting the possibility that sulfur insertion may not precede methyl transfer as had been suggested previously.[52]

Gel-filtration studies using two differentially radiolabeled forms of SAM were also conducted with *Tm* MiaB. When *Tm* MiaB (3 nmol) was incubated for 2 h with [*methyl*-$^{14}$C]SAM and then subjected to AGFC, two peaks of radioactivity were observed: an early peak containing the protein fraction and a later peak containing only small molecules (Figure 4B). From the specific radioactivity of SAM, it was calculated that 3.3 nmol of radioactivity was attached to the protein, which represents a stoichiometry of ~1.1. This stoichiometry is consistent with the aforementioned observation that ~0.9 equiv of SAH is formed per equivalent of *Tm* MiaB polypeptide under similar reaction conditions (Figure 3C). More importantly, when this fraction was analyzed by HPLC, radioactivity was not observed to elute with unreacted SAM or any derivative of SAM (Figure S3A in the Supporting Information), suggesting that the radioactivity was derived from a methyl group transferred to some acceptor on the protein. As shown in Figure 4C, when AGFC was conducted in GFB containing 0.2 N NaOH, no radioactivity eluted with the protein fraction, consistent with attachment of the methyl group to a species that is unstable under very basic conditions. Figure 4A displays the elution profile of [*methyl*-$^{14}$C]SAM in the absence of *Tm* MiaB, showing where small molecules elute during AGFC.

In a separate experiment, *Tm* MiaB was incubated for 2 h at 37 °C with [*methyl*-$^{14}$C]SAM in the absence of substrate and dithionite and then subjected to AGFC. The protein fraction (22.7 nmol of radioactivity), which contained 57% of the expected radioactivity, was treated with 50 mM $H_2SO_4$ (final concentration), and a fraction of the supernatant obtained after centrifugation was analyzed by HPLC with radiometric detection. As shown in Figure S3A in the Supporting Information, very little radioactivity was found in peaks corresponding to SAM, 5′-dA, SAH, adenine, or MTA, and no other significant peaks of radioactivity were found in any other region of the chromatogram. When a similar experiment

was conducted with [*adenosyl*-$^{14}$C]SAM, the vast majority (0.37 nmol) of the radioactivity eluted with the SAH standard (Figure S3B). These results are consistent with a scenario in which the methyl group is transferred to an acid- or base-labile acceptor, which upon treatment with acid (in preparation for HPLC) affords a volatile species.

***Tm* MiaB- and *Tm* RimO-Catalyzed Formation of Methanethiol.** SAH is not a typical degradation product of SAM; its formation at significant rates requires enzymatic assistance.[39] The results described above suggest that *Tm* RimO and *Tm* MiaB catalyze (i) adventitious attack of a water molecule on the activated methyl group of SAM or (ii) transfer of the methyl group from SAM to perhaps one of the bridging $\mu$-sulfido ions (or an externally ligated sulfide ion) of, most probably, the N-terminal [4Fe−4S] cluster. In the former case, methanol would be produced and would need to be tightly bound to the enzymes to survive gel filtration. In the latter case, methanethiol ($CH_3SH$) would be produced after treatment of the methylated enzyme with acid or base. Under acidic conditions, $CH_3SH$ is volatile, which would explain our inability to detect it radiometrically in our HPLC chromatograms of acid-quenched samples. Figure S4 in the Supporting Information shows chromatograms of varying concentrations of methanol analyzed by GC/MS. As can be observed, the limit of detection of methanol was significantly less than 8 $\mu$M. When *Tm* RimO (67 $\mu$M) or *Tm* MiaB (100 $\mu$M) was incubated with SAM for 2 h in the absence of substrate and dithionite to allow for methyl transfer, methanol was not detected in either the liquid or gas phase upon GC/MS analysis of the reaction mixture after the reaction was quenched in either acid or base.

GC/MS was also used to detect time-dependent $CH_3SH$ formation in assays containing *Tm* RimO or *Tm* MiaB and SAM in the absence of substrate and dithionite. Assays were conducted in septum-sealed vials and quenched in acid at appropriate times. The quenched samples were incubated further at 42 °C to allow equilibration of $CH_3SH$ between the liquid phase and the headspace of the vial before an aliquot of the headspace was removed and analyzed. A standard curve was generated with commercially available sodium methanethiolate ($NaSCH_3$), which was added to reaction mixtures containing all of the components except *Tm* RimO or *Tm* MiaB. The samples used to construct the standard curve were quenched and treated as described above for the experimental samples. In Figure 5, the time-dependent formation of SAH (blue squares) and $CH_3SH$ (red circles) is displayed for reactions containing SAM and 67 $\mu$M *Tm* RimO (Figure 5A) or SAM and 100 $\mu$M *Tm* MiaB (Figure 5B). The lines in each graph are fits of the data to a first-order, single-exponential kinetic equation, which afforded the following amplitudes ($A$) and initial rates ($v$) for SAH and $CH_3SH$ formation, respectively: $A$ = 40 ± 0.8 $\mu$M, $v$ = 4.0 ± 0.1 $\mu$M min$^{-1}$ and 37 ± 2 $\mu$M, $v$ = 3.7 ± 0.2 $\mu$M min$^{-1}$ (*Tm* RimO); $A$ = 47 ± 2 $\mu$M, $v$ = 1.2 ± 0.2 $\mu$M min$^{-1}$ and 51 ± 2 $\mu$M, $v$ = 1.3 ± 0.2 $\mu$M min$^{-1}$ (*Tm* MiaB). As can be observed, $CH_3SH$ formation closely parallels SAH formation in amplitude and initial rate both for *Tm* RimO and *Tm* MiaB.

**Turnover in the Presence of Exogenously Supplied Methanethiol.** To assess whether the methylated sulfur ion is in exchange with free $CH_3SH$ in catalysis by *Tm* RimO (67 $\mu$M), reactions were conducted with unlabeled SAM or $d_3$-SAM in the absence or presence of $NaSCH_3$. In Figure 6A, the *Tm* RimO-catalyzed time-dependent production of MS-**1** in the presence of SAM (2 mM), **1** (300 $\mu$M), and $NaSCH_3$ (1 mM) is displayed (black line). As can be observed, in the presence of

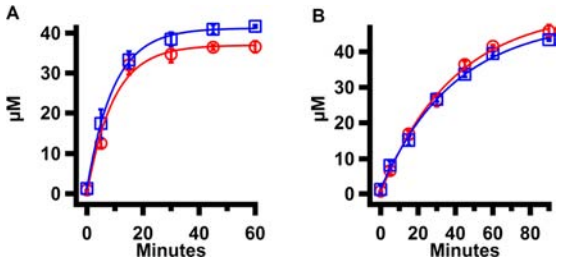


**Figure 5.** Time-dependent formation of SAH and methanethiol by *Tm* RimO and *Tm* MiaB. Each reaction was performed in triplicate. The dashed lines are fits to a first-order single-exponential kinetic equation: (A) SAH formation by *Tm* RimO: $A$ = 40 ± 0.8 $\mu$M, $v$ = 4.0 ± 0.1 $\mu$M min$^{-1}$ (blue squares); methanethiol formation by *Tm* RimO: $A$ = 37 ± 2 $\mu$M, $v$ = 3.7 ± 0.2 $\mu$M min$^{-1}$ (red circles); (B) SAH formation by *Tm* MiaB: $A$ = 47 ± 2 $\mu$M, $v$ = 1.2 ± 0.2 $\mu$M min$^{-1}$ (blue squares); methanethiol formation by *Tm* MiaB: $A$ = 51 ± 2.0 $\mu$M, $v$ = 1.2 ± 0.2 $\mu$M min$^{-1}$ (red circles). The reactions were conducted as described in Materials and Methods. The reaction mixtures contained 67 $\mu$M *Tm* RimO or 100 $\mu$M MiaB, 50 mM Na-HEPES (pH 7.5), 1 mM tryptophan, and 1 mM SAM.

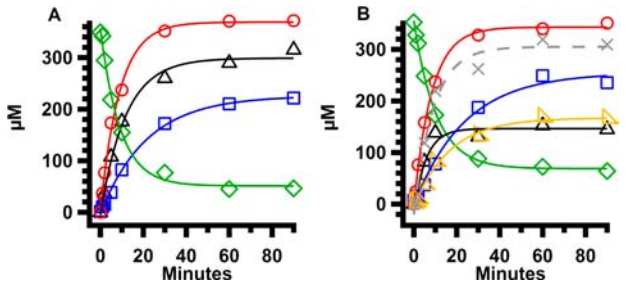


**Figure 6.** (A) Time-dependent formation of MS-**1** in the presence of 1 mM methanethiol and 2 mM SAM. (B) Time-dependent formation of MS-**1** and $d_3$-MS-**1** in the presence of 2 mM methanethiol and 2 mM $d_3$-SAM. SAH formation (blue squares), 5′-dA formation (red circles), MS-**1** formation (black triangles), $d_3$-MS-**1** formation (yellow right triangles), MS-**1** + $d_3$-MS-**1** formation (gray crosses), and consumption of **1** (green diamonds). The reactions were conducted as described in Materials and Methods. Both reaction mixtures contained 67 $\mu$M *Tm* RimO, 50 mM Na-HEPES (pH 7.5), 1 mM tryptophan, 2 mM dithionite, and 350 $\mu$M **1**. The lines are fits to a first-order single-exponential equation with the following obtained parameters: (A) SAH formation: $A$ = 228 ± 4 $\mu$M, $v$ = 10.5 ± 0.2 $\mu$M min$^{-1}$; 5′-dA formation: $A$ = 367 ± 8 $\mu$M, $v$ = 40.4 ± 0.9 $\mu$M min$^{-1}$; MS-**1** formation: $A$ = 304 ± 11 $\mu$M, $v$ = 25.8 ± 0.9 $\mu$M min$^{-1}$; consumption of **1**: $A$ = 306 ± 11 $\mu$M, $v$ = 33.7 ± 1.2 $\mu$M min$^{-1}$. (B) SAH formation: $A$ = 257 ± 13 $\mu$M, $v$ = 10.8 ± 0.5 $\mu$M min$^{-1}$ ; 5′-dA formation: $A$ = 347 ± 7 $\mu$M, $v$ = 41.6 ± 0.8 $\mu$M min$^{-1}$; $d_3$-MS-**1** formation: $A$ = 172 ± 6 $\mu$M, $v$ = 10.3 ± 0.4 $\mu$M min$^{-1}$; MS-**1** formation: $A$ = 164 ± 16 $\mu$M, $v$ = 29.5 ± 2.9 $\mu$M min$^{-1}$; formation of MS-**1** + $d_3$-MS-**1**: $A$ = 325 ± 21 $\mu$M, $v$ = 35.8 ± 2.3 $\mu$M min$^{-1}$; consumption of **1**: $A$ = 287 ± 4 $\mu$M, $v$ = 27.3 ± 0.4 $\mu$M min$^{-1}$.

$NaSCH_3$, *Tm* RimO catalyzed multiple turnovers (~4.5 per polypeptide). Moreover, the initial rate for MS-**1** formation (25.8 ± 0.9 $\mu$M min$^{-1}$) was increased by a factor of ~4 over that observed in reactions lacking $NaSCH_3$ (5.8 ± 0.3 $\mu$M min$^{-1}$; Figure 1A), while the initial rates for SAH formation in the two reactions were similar (10.5 ± 0.2 vs 11.9 ± 0.7 $\mu$M min$^{-1}$, respectively). The observation that the initial rate for formation of SAH is on the order of that for formation of MS-**1** in the absence of $NaSCH_3$ suggests that methyl transfer from SAM to the acceptor may limit or partially limit the rate of the reaction. The faster initial rate of product formation in assays


dx.doi.org/10.1021/ja4048448 | J. Am. Chem. Soc. 2013, 135, 15404−15416

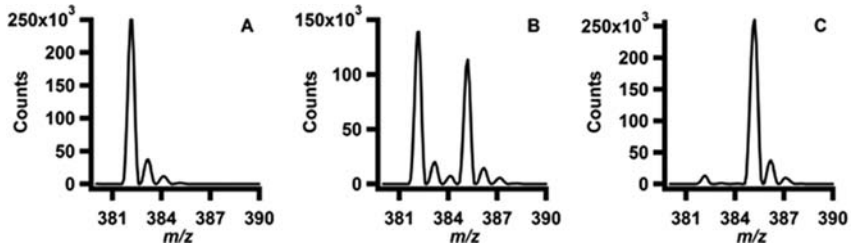


**Figure 7.** Isotopic distributions of $ms^2i^6A$ in assays containing 20 $\mu$M *Tm* MiaB, 100 $\mu$M $i^6A$ ACSL RNA substrate, and 1 mM dithionite in the presence of (A) 500 $\mu$M SAM, (B) 500 $\mu$M $d_3$-SAM + 500 $\mu$M $NaSCH_3$, or (C) 500 $\mu$M $d_3$-SAM. After 2 h at 37 °C, (A) 19.4 $\mu$M $ms^2i^6A$ was generated in the presence of SAM only, (B) 11.7 $\mu$M $ms^2i^6A$ and 9.8 $\mu$M $d_3$-$ms^2i^6A$ were generated in the presence both of SAM and $NaSCH_3$, and (C) 21.2 $\mu$M $d_3$-$ms^2i^6A$ was generated in the presence of $d_3$-SAM only.

containing $NaSCH_3$ suggests that the small molecule is efficiently incorporated into a binding site on the enzyme.

To show convincingly that a methylthio group from $NaSCH_3$ was incorporated into the product during turnover, *Tm* RimO assays were conducted with $d_3$-SAM (2 mM) in the presence (2 mM) and absence of $NaSCH_3$. Product arising from the natural endogenous pathway should contain a deuterated methyl group derived from $d_3$-SAM, while product arising from the exogenous pathway should contain an unlabeled methyl group derived from $NaSCH_3$. In Figure 6B, the *Tm* RimO (67 $\mu$M)-catalyzed time-dependent production of unlabeled ($-SCH_3$) MS-**1** (black trace), labeled ($-SCD_3$) MS-**1** (yellow trace), SAH (blue trace), and 5′-dA (red trace) are displayed along with the time-dependent loss of **1** (green trace). As can be seen, the initial production of unlabeled MS-**1** (29.5 ± 2.9 $\mu$M $min^{-1}$) is faster than that of labeled MS-**1** (10.3 ± 0.4 $\mu$M $min^{-1}$); however, the labeled and unlabeled species are produced in approximately equimolar concentrations ($A$ = 164 ± 16 $\mu$M and 172 ± 6 $\mu$M, respectively). It appears that for the production of labeled MS-**1**, the rate-limiting step is methyl transfer, as SAH was produced with a similar initial rate ($v$ = 10.8 ± 0.5 $\mu$M $min^{-1}$). The gray trace in Figure 6B is the sum of the black and yellow traces; it mirrors red trace corresponding to 5′-dA production both in amplitude (325 ± 21 vs 347 ± 7 $\mu$M) and initial rate (41.6 ± 0.8 vs 35.8 ± 2.3 $\mu$M $min^{-1}$), consistent with the generation of both unlabeled and labeled products via a radical-dependent process and tighter coupling of radical generation and product formation in the presence of methanethiol. Figure S5 in the Supporting Information shows the black and yellow traces only, allowing for better visualization of th eproduction of the two differentially labeled products at early time points.

Figure 7 depicts the results of single-time-point reactions (2 h at 37 °C) in which *Tm* MiaB (20 $\mu$M) was incubated with unlabeled SAM (Figure 7A), $d_3$-SAM (Figure 7C), or $d_3$-SAM (500 $\mu$M) + $NaSCH_3$ (500 $\mu$M) (Figure 7B). In contrast to similar reactions with *Tm* RimO, the addition of $NaSCH_3$ to the *Tm* MiaB reactions did not significantly enhance the extent of turnover. After 2 h at 37 °C, 19 $\mu$M $ms^2i^6A$ was generated with unlabeled SAM and 21 $\mu$M $d_3$-$ms^2i^6A$ was generated with $d_3$-SAM, while 12 $\mu$M $ms^2i^6A$ and 10 $\mu$M $d_3$-$ms^2i^6A$ were generated in the reaction containing both $d_3$-SAM and $NaSCH_3$. Interestingly, as observed for the *Tm* RimO reaction when both $NaSCH_3$ and $d_3$-SAM were present, the unlabeled and labeled products were generated in approximately equal concentrations. These results show that *Tm* MiaB, like *Tm* RimO, can use exogenously supplied $NaSCH_3$ as the source of the methylthio group introduced into $ms^2i^6A$, suggesting a similarity in the mechanisms of the two enzymes.

**Chemical and Kinetic Competence of a Potential Intermediate.** If *Tm* RimO and *Tm* MiaB follow ping-pong mechanisms, it should be possible to isolate the intermediate form of the protein after incubation of the protein with the first substrate in the reaction (the "ping" step) and then reintroduce the intermediate form into a reaction containing only the second substrate (the "pong" step). One caveat of this common method to show chemical competence is that in the MTTases, the same cosubstrate (SAM) is required in both steps of the reaction. However, the finding that SAM is used for distinctly different types of reactivities in the two steps, one of which requires the presence of a low-potential reductant (dithionite), allowed differentiation of the two steps by omission of the low-potential reductant required to initiate the radical chemistry. Therefore, the first step, methylation of an acceptor, was conducted with unlabeled SAM in the absence of dithionite, while the second step, radical-dependent introduction of a methylthio group into the organic substrate, was conducted with $d_3$-SAM in the presence of dithionite. Figure 8 displays the results of these differential labeling experiments with *Tm* RimO, wherein the protein was treated with excess SAM for 15 h and then subjected to AGFC before it was incubated with $d_3$-SAM, dithionite, and **1** (turnover conditions). Figure 8A displays the time-dependent formation of MS-**1** (black triangles), $d_3$-MS-**1** (yellow triangles), SAH (blue squares), and 5′-dA (red circles) as well as the time-dependent loss of **1** (green squares) for a sample that was incubated with $d_3$-SAM for 3 min before addition of **1** and dithionite (in that order) to initiate the reaction. Formation of unlabeled MS-**1** occurred relatively rapidly ($v$ = 21.2 ± 1.4 $\mu$M $min^{-1}$); however, the concentration of unlabeled MS-**1** reached a plateau at ∼50 $\mu$M (0.75 equiv of enzyme). Formation of $d_3$-MS-**1** occurred with a lag phase, implying a slow step that precedes $d_3$-MS-**1** formation, which may involve methyl transfer, dissociation of SAH, and rebinding of another molecule of SAM needed for radical generation. Figure S6 in the Supporting Information displays only the black and yellow curves, better revealing the pronounced lag associated with $d_3$-MS-**1** formation. In addition, this labeled product was produced in a 2-fold greater amount (∼100 $\mu$M) than the unlabeled product after 30 min of reaction time. Figure 8B,C displays the results of repeats of the experiment described in Figure 8A in which the intermediate form of *Tm* RimO was incubated with $d_3$-SAM for 1 and 3 h, respectively, before the second phase of the reaction was initiated by introduction of **1** and dithionite. As can be observed, these extended incubation times had no significant effect on the distribution of the labeled and unlabeled MS-**1** products, indicating that exchange between the methylated acceptor and the methyl group of SAM does not take place and that the


dx.doi.org/10.1021/ja4048448 | J. Am. Chem. Soc. 2013, 135, 15404−15416

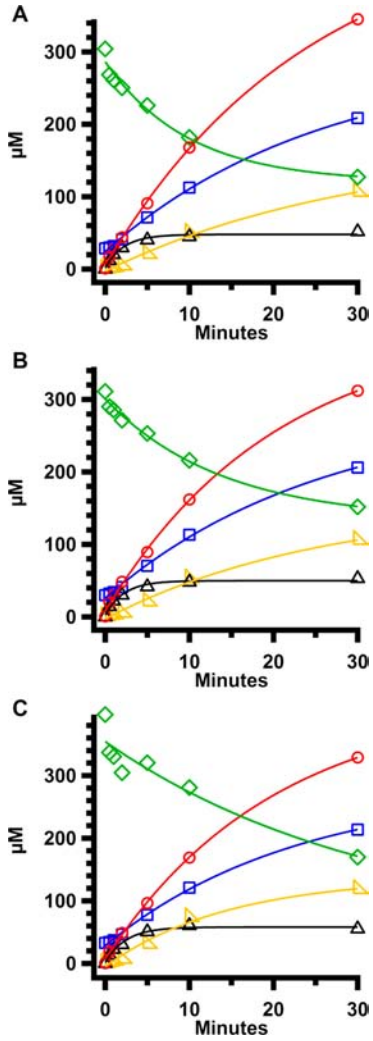


**Figure 8.** Time courses for the formation of 5′-dA (red circles), SAH (blue squares), MS-**1** (black triangles), and $d_3$-MS-**1** (yellow right triangles) and the consumption of **1** (green diamonds) by *Tm* RimO incubated with $d_3$-SAM for (A) 3 min, (B) 1 h, and (C) 3 h after previous incubation with unlabeled SAM for 15 h followed by AGFC. The lines are fits to a first-order single-exponential equation with the following obtained kinetic parameters for formation of MS-**1** and $d_3$-MS-**1**, respectively: (A) $A$ = 47 ± 3.0 μM, $v$ = 21.2 ± 1.4 μM min$^{-1}$ and $A$ = 174 ± 31 μM, $v$ = 5.7 ± 1.0 μM min$^{-1}$; (B) $A$ = 47 ± 3 μM, $v$ = 21.2 ± 1.4 μM min$^{-1}$ and $A$ = 159 ± 26 μM, $v$ = 6.0 ± 1.0 μM min$^{-1}$; (C) $A$ = 56 ± 3 μM, $v$ = 23.0 ± 1.2 μM min$^{-1}$ and $A$ = 142 ± 14 μM, $v$ = 9.8 ± 1.0 μM min$^{-1}$. Reactions were conducted as described in Materials and Methods and contained 67 μM RimO, 50 mM Na-HEPES (pH 7.5), 1 mM tryptophan, 300 μM **1**, and 1 mM $d_3$-SAM.

methyl donor in the second step of the reaction is not a bound molecule of SAM that survived AGFC.

A similar experiment was conducted with *Tm* MiaB; however, the protein was not subjected to AGFC between the two half-reactions. Instead, in the first half-reaction, *Tm* MiaB (150 μM) was incubated at 37 °C with an equal concentration of unlabeled SAM until all of the SAM was converted to SAH. In the second half-reaction, $d_3$-SAM (500 μM final concentration) and the ACSL substrate (130 μM final concentration) were added to the reaction mixture to give a final *Tm* MiaB concentration of 100 μM, and the reaction was initiated by addition of dithionite after 3 min of preincubation. Figure 9A shows that in the first half-reaction, ∼110 μM SAH was formed (blue squares), suggesting that ∼0.7 equiv of

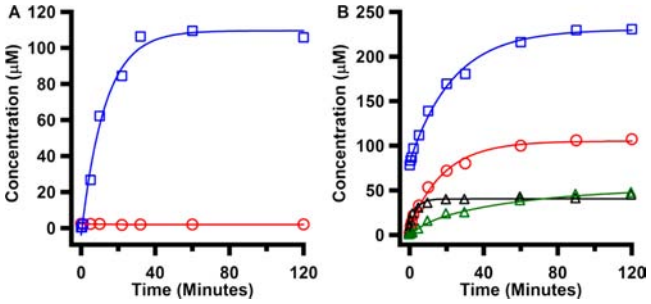


**Figure 9.** Time courses for the formation of SAH (blue triangles), 5′-dA (red circles), ms$^2$i$^6$A (black triangles), and $d_3$-ms$^2$i$^6$A (green triangles) upon (A) initial incubation of 150 μM *Tm* MiaB with a stoichiometric concentration of SAM in the absence of dithionite followed by (B) introduction of excess (500 μM) $d_3$-SAM, 130 μM i$^6$A ACSL RNA, and 1 mM dithionite in 50 mM Tris-HCl pH 7.5. The lines are fits to a first-order single-exponential equation with the following obtained kinetic parameters: (A) SAH formation: $A$ = 110 ± 4 μM, $v$ = 8.5 ± 1.3 min$^{-1}$; (B) 5′-dA formation: $A$ = 105 ± 3 μM, $v$ = 5.7 ± 0.7 μM min$^{-1}$; SAH formation: $A$ = 230 ± 3 μM, $v$ = 9.7 ± 0.8 μM min$^{-1}$; ms$^2$i$^6$A formation: $A$ = 40 ± 1 μM, $v$ = 11.6 ± 2.6 μM min$^{-1}$; $d_3$-ms$^2$i$^6$A formation: $A$ = 48 ± 2 μM, $v$ = 1.3 ± 0.2 μM min$^{-1}$.

enzyme had reacted. Because the protein was not subjected to AGFC between the two half-reactions, the apparent burst of SAH formation in Figure 9B (blue squares) derived from the SAH produced after the first step (Figure 9A) after accounting for a 1.5-fold dilution to bring the concentration of *Tm* MiaB to 100 μM. Also displayed in Figure 9B is the formation of unlabeled ms$^2$i$^6$A (black triangles), $d_3$-ms$^2$i$^6$A (green triangles), and 5′-dA (red circles) during the second half-reaction under turnover conditions. Similar to the reaction catalyzed by *Tm* RimO, the initial rate for formation of unlabeled ms$^2$i$^6$A ($v$ = 11.6 ± 2.6 μM min$^{-1}$) was significantly (∼10-fold) greater than that for formation of $d_3$-ms$^2$i$^6$A ($v$ = 1.3 ± 0.2 μM min$^{-1}$), although the two species appeared to be formed in approximately equal amounts. Figure S7 in the Supporting Information displays only the black and green curves, better revealing the pronounced lag associated with $d_3$-ms$^2$i$^6$A formation. It should be noted that the rate of formation of $d_3$-ms$^2$i$^6$A was similar to the rate of formation of SAH in Figure 3, suggesting again that methyl transfer may limit or partially limit the rate of these MTTase reactions. Cumulatively, these results are consistent with a mechanism wherein a methyl group from SAM is transferred to a sulfur ion (presumably located on one of the [4Fe−4S] clusters) by an $S_N2$ mechanism, which is followed by a radical-dependent transfer of an intact methylthio group from the protein to the substrate. On the basis of the amount of SAH formed in the initial methylation of the protein, it would appear that only half of the methylated sites were actually used to donate the methylthio group, as there was about a 2:1 ratio of SAH to the unlabeled methylated product. Upon transfer of this methylthio group, the same sites become available for one or two more rounds of methyl transfer and subsequent methylthiolation.

## DISCUSSION

Previous in vivo studies on *Ec* MiaB led to the suggestion that the sequence of methylthiolation involves initial sulfhydrylation of the substrate followed by capping of the sulfur atom with a


dx.doi.org/10.1021/ja4048448 | J. Am. Chem. Soc. 2013, 135, 15404−15416

**Scheme 2. Working Hypothesis for the Reaction Catalyzed by *Tm* RimO[a]**

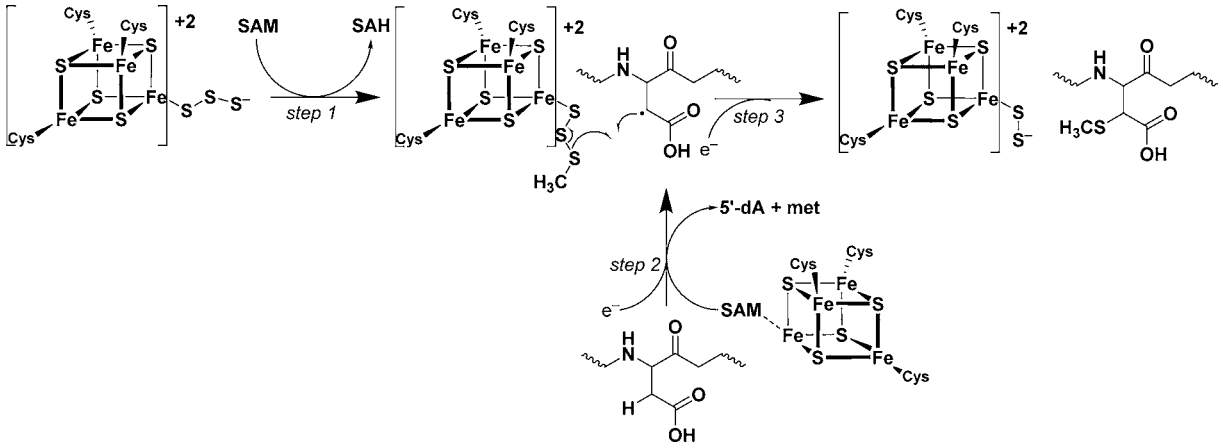


[a]Step 1: transfer of a methyl group from SAM bound to the RS [4Fe−4S] cluster to the external sulfur ion of a polysulfide group attached to the unique iron ion of the auxiliary [4Fe−4S] cluster. Step 2: reductive fragmentation of a second molecule of SAM bound to the RS [4Fe−4S] cluster to give 5′-dA· and abstraction of H· from the bound substrate. Step 3: attack of a substrate radical on the methylated sulfur atom of the polysulfide chain to afford the methylthiolated product and a $[4Fe{-}4S]^{2+}$ cluster with a terminal persulfide.

SAM-derived methyl group.[54] Starvation of an *Ec* (*rel met cys*) mutant for methionine (a precursor to SAM), but not cysteine, resulted in the trapping of a cytokinin-active species suspected to be 2-thio-$N^6$-($\Delta^2$-isopentenyl)adenosine ($s^2i^6A$), as its treatment with [*methyl*-$^{14}$C]SAM and a crude MiaB preparation resulted in incorporation of radioactivity into the species. The observation that the species was cytokinin-active suggested that it contained a dimethylallyl group, and the observation that radioactivity from [*methyl*-$^{14}$C]SAM was not incorporated into tRNA isolated from *Ec* mutants starved for sulfur (cysteine or sulfate) lent credibility to its assignment as $s^2i^6A$.[54]

The MTTases represent one of a few classes of enzymes wherein a single polypeptide directs two distinct chemical outcomes for SAM: reductive cleavage to give 5′-dA· and $S_N2$-based methyl transfer to an acceptor, affording SAH as a coproduct. In the best studied class, represented by the RS methylases RlmN and Cfr, which catalyze the synthesis of methyl groups at C2 and C8, respectively, of adenosine 2503 of 23*S* rRNA, catalysis takes place via a ping-pong-like mechanism involving an initial $S_N2$-based transfer of a methyl group to a target Cys residue before it is transferred to the nucleotide substrate via radical-dependent chemistry.[34,38] The studies detailed herein provide strong evidence for an analogous ping-pong-like mechanism for MTTases. As we observed for *Ec* RimO,[12] both *Tm* RimO and *Tm* MiaB catalyze the formation of SAH from SAM in the absence of substrate and/or dithionite, a reductant with a suitably low redox potential to initiate radical-dependent chemistry. In the absence both of substrate and dithionite, the formation of SAH follows hyperbolic kinetics, with the maximum concentration generated approaching the concentration of enzyme in the reaction. Our results are consistent with the transfer of a methyl group from SAM to an acceptor on the protein that is labile in the presence of acid and base and moderately labile in the presence of chaotropic agents such as urea. The lability of the acceptor in the presence of agents that denature the overall fold of the protein suggests that the acceptor is most likely not an amino acid residue whose methylated side chain can be hydrolyzed in the presence of acid or base (e.g., methyl glutamate or methyl aspartate), and our inability to detect methanol after denaturation of the protein under acidic or basic conditions indicates that the acceptor is not a tightly bound water molecule. Indeed, subsequent to treatment of *Tm* RimO or *Tm* MiaB with SAM in the absence of dithionite and denaturation of the proteins in acid, methanethiol was produced in amounts that were stoichiometric with SAH. These results are consistent with a polar ($S_N2$) transfer of a methyl group from SAM to a sulfide ion.

When *Tm* RimO or *Tm* MiaB was incubated with SAM in the presence of dithionite, no 5′-dA was formed unless substrate was present, indicating that radical-dependent chemistry is strongly coupled to substrate binding. However, the presence of dithionite strongly affected the extent to which SAH was formed, with the maximum concentration produced significantly exceeding the concentration of enzyme. Although we do not know the exact basis for the enhanced SAH production in the presence of dithionite, it may derive from reduction of a source of sulfane sulfur that is methylated by SAM, resulting in release of methanethiol. This sulfane sulfur was recently observed in the holo crystal structure of *Tm* RimO, wherein a pentasulfide bridge was observed to connect the unique iron ions of each of the [4Fe−4S] clusters.[16] It should be mentioned that dithionite is not a physiological reductant and that its unspecific reactivity can short-circuit natural catalytic sequences, as has been observed in BS, which also contains two redox-active Fe/S clusters.[8] The *Ec* flavodoxin/flavodoxin reductase/NADPH reducing system appears to be capable of supplying the requisite electron for SAM cleavage in most RS enzymes from *Ec* and some other organisms; however, it was relatively ineffective in our *Tm* RimO and *Tm* MiaB reactions. Previous studies on *Tm* MiaB have shown that the auxiliary cluster has a relatively high redox potential; it is fully reduced upon treatment with dithionite, and the triple variant lacking the cysteines that coordinate the RS cluster is partially reduced simply after isolation and reconstitution.[10] Whether the oxidized or reduced form of the auxiliary cluster functions in the initial stages of the physiological reaction mechanism is currently unknown.

Our results further suggest that the methylated species is a chemically and kinetically competent intermediate in the reaction. Not only was methanethiol produced after incubating *Tm* RimO or *Tm* MiaB with SAM and then denaturing each in


dx.doi.org/10.1021/ja4048448 | *J. Am. Chem. Soc.* 2013, 135, 15404−15416

acid, but also, methanethiol introduced exogenously in reaction mixtures served as a perfectly good methylthiolating agent in the presence of SAM and dithionite, as has recently been demonstrated by others.[16] In fact, in reactions containing $NaSCH_3$ and [*methyl-*$d_3$]SAM, production of unlabeled product was initially favored over the $d_3$-containing product. This observation suggests that exogenous methanethiol is efficiently activated toward radical-dependent incorporation into organic substrates. Moreover, when *Tm* RimO or *Tm* MiaB was first treated with unlabeled SAM in the absence of dithionite to allow for methyl transfer to the target acceptor and then treated with [*methyl-*$d_3$]SAM under turnover conditions, production of the unlabeled product preceded production of the labeled product. This behavior was more dramatic in the *Tm* RimO reaction, wherein a clear lag phase associated with $d_3$-MS-**1** production was observed during the burst phase of MS-**1** production. Not only is this initial methyl-containing species chemically competent for methylthiolation, but also, the initial rate of product formation from the methyl-containing species generated in the first half-reaction ($v = 21.2 \pm 1.4\ \mu M\ min^{-1}$) indicates that it is also kinetically competent. In fact, these differential labeling studies, as well as the studies detailed above using exogenous methanethiol, suggest that methyl transfer from SAM is at least partially rate-limiting in these reactions.

At present, we cannot readily explain the stoichiometry of unlabeled product to labeled product observed in our differential labeling experiments. Before we initiated these experiments, the prediction was that we would observe a maximum of 1 equiv of methylthiolated product per equivalent of MTTase and that the product would bear exclusively an unlabeled methyl group. Surprisingly, in the *Tm* RimO reaction, we observed 0.7 equiv of the unlabeled product while an additional ∼1.4 equiv of the labeled product was formed in a slower process, whereas in the *Tm* MiaB reaction, we observed ∼0.5 equiv of the unlabeled product while another 0.5 equiv was formed in a slower process. The recent crystal structure of holo *Tm* RimO provides possible insight into these findings. On the basis of our observations, it is tempting to speculate that ∼70% of our *Tm* RimO and ∼50% of our *Tm* MiaB react productively and that our RCN *Tm* RimO contains a trisulfide substituent coordinated to the unique iron ion of the auxiliary cluster (Scheme 2) while our *Tm* MiaB contains a disulfide substituent in the corresponding location. In the *Tm* RimO reaction, we suggest that methyl transfer from SAM to the external sulfide ion of the polysulfide substituent takes place via polar $S_N2$-based chemistry, most likely from SAM bound to the RS [4Fe−4S] cluster. Upon reductive cleavage of SAM and abstraction of H· from the substrate by the resulting 5′-dA·, the substrate radical attacks the terminal sulfur atom of the polysulfide chain attached to the auxiliary cluster in its reduced state, resulting in transfer of the methylthiol group to afford the product. This reaction produces a polysulfide chain that is shorter by one sulfur atom but bears a nucleophilic terminal persulfide for another round of the exact same chemistry (Scheme 2). This proposed reaction mechanism, wherein SAM bound to the RS [4Fe−4S] cluster is activated toward two distinct types of chemistry, is also consistent with the relatively short distance between the two Fe/S clusters (∼8 Å) in comparison with those in MoaA (17 Å)[55] and the recently solved structure of the anaerobic sulfatase maturating enzyme from *Clostridium perfringens* (12.9 Å).[56]

Recent studies suggest that a similar ping-pong-like mechanism may be operative in the reaction catalyzed by the RS enzyme NifB. This enzyme plays a key role in the maturation of the M cluster of Mo-nitrogenase, the metalloenzyme responsible for reduction of $N_2$ to ammonia. Mo-nitrogenase contains a complex metallocluster with core composition 1Mo:7Fe:9S:C. At the center of this metallocluster is a carbide atom coordinated to six iron ions that emanates from the activated methyl group of SAM.[57−60] Treatment of a NifEN-B fusion protein (in which NifB is fused to the scaffold proteins NifEN) with SAM under turnover conditions results in the production both of 5′-dA and SAH. Further labeling experiments with $d_3$-SAM showed deuterium enrichment in 5′-dA, as was observed in the reactions catalyzed by RlmN and Cfr.[34,35] The authors proposed a mechanism involving initial transfer of a methyl group from SAM to some atom on a precursor to the M-cluster followed by abstraction of at least one H· by a 5′-dA· generated via reductive cleavage of another molecule of SAM.[60] It appears that ping-pong-like mechanisms for RS methylation reactions may be relatively common.

## ■ ASSOCIATED CONTENT

### Ⓢ Supporting Information

Figures S1−S7. This material is available free of charge via the Internet at http://pubs.acs.org.

## ■ AUTHOR INFORMATION


### Corresponding Author

Squire@psu.edu

### Author Contributions

[§]B.J.L. and A.J.A. contributed equally.


### Notes

The authors declare no competing financial interest.

## ■ ACKNOWLEDGMENTS

S.J.B. gratefully acknowledges NIH (GM-63847 and GM-103268) for support of this work.

## ■ REFERENCES


(1) Atta, M.; Mulliez, E.; Arragain, S.; Forouhar, F.; Hunt, J. F.; Fontecave, M. *Curr. Opin. Struct. Biol.* **2010**, *20*, 1.

(2) Anton, B. P.; Russell, S. P.; Vertrees, J.; Kasif, S.; Raleigh, E. A.; Limbach, P. A.; Roberts, R. J. *Nucleic Acids Res.* **2010**, *38*, 6195.

(3) Arragain, S.; García-Serres, R.; Blondin, G.; Douki, T.; Clemancey, M.; Latour, J.-M.; Forouhar, F.; Neely, H.; Montelione, G. T.; Hunt, J. F.; Mulliez, E.; Fontecave, M.; Atta, M. *J. Biol. Chem.* **2010**, *285*, 5792.

(4) Booker, S. J.; Cicchillo, R. M.; Grove, T. L. *Curr. Opin. Chem. Biol.* **2007**, *11*, 543.

(5) Challand, M. R.; Driesener, R. C.; Roach, P. L. *Nat. Prod. Rep.* **2011**, *28*, 1696.

(6) Frey, P. A.; Hegeman, A. D.; Ruzicka, F. J. *Crit. Rev. Biochem. Mol. Biol.* **2008**, *43*, 63.

(7) Cosper, M. M.; Jameson, G. N. L.; Hernández, H. L.; Krebs, C.; Huynh, B. H.; Johnson, M. K. *Biochemistry* **2004**, *43*, 2007.

(8) Ugulava, N. B.; Gibney, B. R.; Jarrett, J. T. *Biochemistry* **2001**, *40*, 8343.

(9) Ugulava, N. B.; Surerus, K. K.; Jarrett, J. T. *J. Am. Chem. Soc.* **2002**, *124*, 9050.

(10) Hernández, H. L.; Pierrel, F.; Elleingand, E.; García-Serres, R.; Huynh, B. H.; Johnson, M. K.; Fontecave, M.; Atta, M. *Biochemistry* **2007**, *46*, 5140.

(11) Cicchillo, R. M.; Lee, K.-H.; Baleanu-Gogonea, C.; Nesbitt, N. M.; Krebs, C.; Booker, S. J. *Biochemistry* **2004**, *43*, 11770.

(12) Lee, K.-H.; Saleh, L.; Anton, B. P.; Madinger, C. L.; Benner, J. S.; Iwig, D. F.; Roberts, R. J.; Krebs, C.; Booker, S. J. *Biochemistry* **2009**, *48*, 10162.

(13) Walsby, C. J.; Ortillo, D.; Yang, J.; Nnyepi, M. R.; Broderick, W. E.; Hoffman, B. M.; Broderick, J. B. *Inorg. Chem.* **2005**, *44*, 727.
(14) Vey, J. L.; Drennan, C. L. *Chem. Rev.* **2011**, *111*, 2487.
(15) Fugate, C. J.; Stich, T. A.; Kim, E. G.; Myers, W. K.; Britt, R. D.; Jarrett, J. T. *J. Am. Chem. Soc.* **2012**, *134*, 9042.
(16) Forouhar, F.; Arragain, S.; Atta, M.; Gambarelli, S.; Mouesca, J.-M.; Hussain, M.; Xiao, R.; Kieffer-Jaquinod, S.; Seetharaman, J.; Acton, T. B.; Montelione, G. T.; Mulliez, E.; Hunt, J. F.; Fontecave, M. *Nat. Chem. Biol.* **2013**, *9*, 333.
(17) Bartz, J. K.; Kline, L. K.; Soll, D. *Biochem. Biophys. Res. Commun.* **1970**, *40*, 1481.
(18) Caillet, J.; Droogmans, L. *J. Bacteriol.* **1988**, *170*, 4147.
(19) Rosenbaum, N.; Gefter, M. L. *J. Biol. Chem.* **1972**, *247*, 5675.
(20) Elkins, B. N.; Keller, E. B. *Biochemistry* **1974**, *13*, 4622.
(21) Deutsch, C.; El Yacoubi, B.; de Crecy-Lagard, V.; Iwata-Reuyl, D. *J. Biol. Chem.* **2012**, *287*, 13666.
(22) Connolly, D. M.; Winkler, M. E. *J. Bacteriol.* **1989**, *171*, 3233.
(23) Connolly, D. M.; Winkler, M. E. *J. Bacteriol.* **1991**, *173*, 1711.
(24) Esberg, B.; Björk, G. R. *J. Bacteriol.* **1995**, *177*, 1967.
(25) Urbonavicius, J.; Qian, Q.; Durand, J. M. B.; Hagervall, T. G.; Björk, G. R. *EMBO J.* **2001**, *20*, 4863.
(26) Dehwah, M. A.; Wang, M.; Huang, Q. Y. *Genet. Mol. Res.* **2010**, *9*, 1109.
(27) Saxena, R.; Voight, B. F.; Lyssenko, V.; Burtt, N. P.; de Bakker, P. I.; Chen, H.; Roix, J. J.; Kathiresan, S.; Hirschhorn, J. N.; Daly, M. J.; Hughes, T. E.; Groop, L.; Altshuler, D.; Almgren, P.; Florez, J. C.; Meyer, J.; Ardlie, K.; Bengtsson Boström, K.; Isomaa, B.; Lettre, G.; Lindblad, U.; Lyon, H. N.; Melander, O.; Newton-Cheh, C.; Nilsson, P.; Orho-Melander, M.; Råstam, L.; Speliotes, E. K.; Taskinen, M. R.; Tuomi, T.; Guiducci, C.; Berglund, A.; Carlson, J.; Gianniny, L.; Hackett, R.; Hall, L.; Holmkvist, J.; Laurila, E.; Sjögren, M.; Sterner, M.; Surti, A.; Svensson, M.; Tewhey, R.; Blumenstiel, B.; Parkin, M.; Defelice, M.; Barry, R.; Brodeur, W.; Camarata, J.; Chia, N.; Fava, M.; Gibbons, J.; Handsaker, B.; Healy, C.; Nguyen, K.; Gates, C.; Sougnez, C.; Gage, D.; Nizzari, M.; Gabriel, S. B.; Chirn, G. W.; Ma, Q.; Parikh, H.; Richardson, D.; Ricke, D.; Purcell, S. *Science* **2007**, *316*, 1331.
(28) Scott, L. J.; Mohlke, K. L.; Bonnycastle, L. L.; Willer, C. J.; Li, Y.; Duren, W. L.; Erdos, M. R.; Stringham, H. M.; Chines, P. S.; Jackson, A. U.; Prokunina-Olsson, L.; Ding, C. J.; Swift, A. J.; Narisu, N.; Hu, T.; Pruim, R.; Xiao, R.; Li, X. Y.; Conneely, K. N.; Riebow, N. L.; Sprau, A. G.; Tong, M.; White, P. P.; Hetrick, K. N.; Barnhart, M. W.; Bark, C. W.; Goldstein, J. L.; Watkins, L.; Xiang, F.; Saramies, J.; Buchanan, T. A.; Watanabe, R. M.; Valle, T. T.; Kinnunen, L.; Abecasis, G. R.; Pugh, E. W.; Doheny, K. F.; Bergman, R. N.; Tuomilehto, J.; Collins, F. S.; Boehnke, M. *Science* **2007**, *316*, 1341.
(29) Steinthorsdottir, V.; Thorleifsson, G.; Reynisdottir, I.; Benediktsson, R.; Jonsdottir, T.; Walters, G. B.; Styrkarsdottir, U.; Gretarsdottir, S.; Emilsson, V.; Ghosh, S.; Baker, A.; Snorradottir, S.; Bjarnason, H.; Ng, M. C.; Hansen, T.; Bagger, Y.; Wilensky, R. L.; Reilly, M. P.; Adeyemo, A.; Chen, Y.; Zhou, J.; Gudnason, V.; Chen, G.; Huang, H.; Lashley, K.; Doumatey, A.; So, W. Y.; Ma, R. C.; Andersen, G.; Borch-Johnsen, K.; Jorgensen, T.; van Vliet-Ostaptchouk, J. V.; Hofker, M. H.; Wijmenga, C.; Christiansen, C.; Rader, D. J.; Rotimi, C.; Gurney, M.; Chan, J. C.; Pedersen, O.; Sigurdsson, G.; Gulcher, J. R.; Thorsteinsdottir, U.; Kong, A.; Stefansson, K. *Nat. Genet.* **2007**, *39*, 770.
(30) Zeggini, E.; Weedon, M. N.; Lindgren, C. M.; Frayling, T. M.; Elliott, K. S.; Lango, H.; Timpson, N. J.; Perry, J. R.; Rayner, N. W.; Freathy, R. M.; Barrett, J. C.; Shields, B.; Morris, A. P.; Ellard, S.; Groves, C. J.; Harries, L. W.; Marchini, J. L.; Owen, K. R.; Knight, B.; Cardon, L. R.; Walker, M.; Hitman, G. A.; Morris, A. D.; Doney, A. S.; McCarthy, M. I.; Hattersley, A. T. *Science* **2007**, *316*, 1336.
(31) Anton, B. P.; Saleh, L.; Benner, J. S.; Raleigh, E. A.; Kasif, S.; Roberts, R. J. *Proc. Natl. Acad. Sci. U.S.A.* **2008**, *105*, 1826.
(32) Carr, J. F.; Hamburg, D. M.; Gregory, S. T.; Limbach, P. A.; Dahlberg, A. E. *J. Bacteriol.* **2006**, *188*, 2020.
(33) Yan, F.; LaMarre, J. M.; Röhrich, R.; Wiesner, J.; Jomaa, H.; Mankin, A. S.; Galoníc Fujimori, D. *J. Am. Chem. Soc.* **2010**, *132*, 3953.
(34) Grove, T. L.; Benner, J. S.; Radle, M. I.; Ahlum, J. H.; Landgraf, B. J.; Krebs, C.; Booker, S. J. *Science* **2011**, *332*, 604.
(35) Yan, F.; Fujimori, D. G. *Proc. Natl. Acad. Sci. U.S.A.* **2011**, *108*, 3930.
(36) Boal, A. K.; Grove, T. L.; McLaughlin, M. I.; Yennawar, N. H.; Booker, S. J.; Rosenzweig, A. C. *Science* **2011**, *332*, 1089.
(37) Grove, T. L.; Radle, M. I.; Krebs, C.; Booker, S. J. *J. Am. Chem. Soc.* **2011**, *133*, 19586.
(38) McCusker, K. P.; Medzihradszky, K. F.; Shiver, A. L.; Nichols, R. J.; Yan, F.; Maltby, D. A.; Gross, C. A.; Galonic Fujimori, D. *J. Am. Chem. Soc.* **2012**, *134*, 18074.
(39) Iwig, D. F.; Booker, S. J. *Biochemistry* **2004**, *43*, 13496.
(40) Sambrook, J.; Fritsch, E. F.; Maniatis, T. *Molecular Cloning: A Laboratory Manual*, 2nd ed.; Cold Spring Harbor Laboratory Press: Plainview, NY, 1989; Vol. 3.
(41) Cicchillo, R. M.; Iwig, D. F.; Jones, A. D.; Nesbitt, N. M.; Baleanu-Gogonea, C.; Souder, M. G.; Tu, L.; Booker, S. J. *Biochemistry* **2004**, *43*, 6378.
(42) Lanz, N. D.; Grove, T. L.; Gogonea, C. B.; Lee, K. H.; Krebs, C.; Booker, S. J. *Methods Enzymol.* **2012**, *516*, 125.
(43) Bradford, M. *Anal. Biochem.* **1976**, *72*, 248.
(44) Grove, T. L.; Lee, K. H.; St. Clair, J.; Krebs, C.; Booker, S. J. *Biochemistry* **2008**, *47*, 7523.
(45) Beinert, H. *Methods Enzymol.* **1978**, *54*, 435.
(46) Beinert, H. *Anal. Biochem.* **1983**, *131*, 373.
(47) Kennedy, M. C.; Kent, T. A.; Emptage, M.; Merkle, H.; Beinert, H.; Münck, E. *J. Biol. Chem.* **1984**, *259*, 14463.
(48) Soderberg, T.; Poulter, C. D. *Biochemistry* **2000**, *39*, 6546.
(49) Crain, P. F. *Methods Enzymol.* **1990**, *193*, 782.
(50) Ghehrke, C. W.; Kuo, K. C.; McCune, R. A.; Gerhardt, K. O.; Agris, P. F. *J. Chromatogr.* **1982**, *230*, 297.
(51) Johnson, D. C.; Unciuleac, M. C.; Dean, D. R. *J. Bacteriol.* **2006**, *188*, 7551.
(52) Pierrel, F.; Douki, T.; Fontecave, M.; Atta, M. *J. Biol. Chem.* **2004**, *279*, 47555.
(53) Soderberg, T.; Poulter, C. D. *Biochemistry* **2001**, *40*, 1734.
(54) Agris, P. F.; Armstrong, D. J.; Schafer, K. P.; Soll, D. *Nucleic Acids Res.* **1975**, *2*, 691.
(55) Hänzelmann, P.; Schindelin, H. *Proc. Natl. Acad. Sci. U.S.A.* **2004**, *101*, 12870.
(56) Goldman, P. J.; Grove, T. L.; Sites, L. A.; McLaughlin, M. I.; Booker, S. J.; Drennan, C. L. *Proc. Natl. Acad. Sci. U.S.A.* **2013**, *110*, 8519.
(57) Spatzal, T.; Aksoyoglu, M.; Zhang, L.; Andrade, S. L. A.; Schleicher, E.; Weber, S.; Rees, D. C.; Einsle, O. *Science* **2011**, *334*, 940.
(58) Einsle, O.; Tezcan, F. A.; Andrade, S. L. A.; Schmid, B.; Yoshida, M.; Howard, J. B.; Rees, D. C. *Science* **2002**, *297*, 1696.
(59) Lancaster, K. M.; Roemelt, M.; Ettenhuber, P.; Hu, Y.; Ribbe, M. W.; Neese, F.; Bergmann, U.; DeBeer, S. *Science* **2011**, *334*, 974.
(60) Wiig, J. A.; Hu, Y.; Lee, C. C.; Ribbe, M. W. *Science* **2012**, *337*, 1672.